

# Noble Gases: A Record of Earth's Evolution and Mantle Dynamics

Sujoy Mukhopadhyay<sup>1</sup> and Rita Parai<sup>2</sup>

<sup>1</sup>Department of Earth and Planetary Sciences, University of California, Davis, California 95616, USA; email: [sujoy@ucdavis.edu](mailto:sujoy@ucdavis.edu)

<sup>2</sup>Department of Earth and Planetary Sciences, Washington University in St. Louis, St. Louis, Missouri 63130, USA

Annu. Rev. Earth Planet. Sci. 2019. 47:389–419

The *Annual Review of Earth and Planetary Sciences* is online at [earth.annualreviews.org](http://earth.annualreviews.org)

<https://doi.org/10.1146/annurev-earth-053018-060238>

Copyright © 2019 by Annual Reviews.  
All rights reserved

## ANNUAL REVIEWS **CONNECT**

[www.annualreviews.org](http://www.annualreviews.org)

- Download figures
- Navigate cited references
- Keyword search
- Explore related articles
- Share via email or social media

## Keywords

volatiles, noble gases, mantle differentiation, giant impact, magma ocean, atmospheric loss

## Abstract

Noble gases have played a key role in our understanding of the origin of Earth's volatiles, mantle structure, and long-term degassing of the mantle. Here we synthesize new insights into these topics gained from high-precision noble gas data. Our analysis reveals new constraints on the origin of the terrestrial atmosphere, the presence of nebular neon but chondritic krypton and xenon in the mantle, and a memory of multiple giant impacts during accretion. Furthermore, the reservoir supplying primordial noble gases to plumes appears to be distinct from the mid-ocean ridge basalt (MORB) reservoir since at least 4.45 Ga. While differences between the MORB mantle and plume mantle cannot be explained solely by recycling of atmospheric volatiles, injection and incorporation of atmospheric-derived noble gases into both mantle reservoirs occurred over Earth history. In the MORB mantle, the atmospheric-derived noble gases are observed to be heterogeneously distributed, reflecting inefficient mixing even within the vigorously convecting MORB mantle.

- Primordial noble gases in the atmosphere were largely derived from planetesimals delivered after the Moon-forming giant impact.

- Heterogeneities dating back to Earth's accretion are preserved in the present-day mantle.
- Mid-ocean ridge basalts and plume xenon isotopic ratios cannot be related by differential degassing or differential incorporation of recycled atmospheric volatiles.
- Differences in mid-ocean ridge basalts and plume radiogenic helium, neon, and argon ratios can be explained through the lens of differential long-term degassing.

## 1. INTRODUCTION

The noble gases are unique tracers of the sources of volatiles to Earth, the mantle's degassing history, the style of mantle convection, and volatile exchange between Earth's interior and the atmosphere. Isotopic ratios of noble gases are distinct in mid-ocean ridge basalts (MORBs) compared to ocean islands such as Iceland, Hawaii, the Galapagos, Réunion, and Samoa, which are manifestations of mantle plumes (e.g., Farley et al. 1992; Hanyu et al. 2001; Honda et al. 1993; Kurz et al. 1982a,b, 1983; Mukhopadhyay 2012; Poreda & Farley 1992; Raquin & Moreira 2009; Trierloff et al. 2000, 2002; Yokochi & Marty 2004). The differences between plume and MORB signatures have been attributed to plumes sampling a significantly less-degassed lower mantle reservoir and MORBs sampling a more-degassed upper mantle reservoir (e.g., Allègre et al. 1987; Gonnermann & Mukhopadhyay 2009; Graham 2002; Kurz et al. 1983, 2009; Porcelli & Wasserburg 1995; Staudacher & Allègre 1982). However, geodynamic models of whole mantle convection suggest that long-term preservation of a less-degassed lower mantle may be problematic (van Keken & Ballentine 1998, 1999). Consequently, numerous alternative interpretations have been proposed, most of which attempt to explain the differences in mantle helium (He) isotopic compositions within the framework of a plume source that has been highly processed and depleted by mantle convection (e.g., Bouhifd et al. 2013, Holland & Ballentine 2006, Huang et al. 2014, Lee et al. 2010).

The isotopes of neon (Ne), argon (Ar), krypton (Kr), and xenon (Xe) can provide information that is not readily observed in the He isotopic compositions, and they have the power to evaluate the alternative interpretations that assign the He isotopic composition of plumes to a depleted and processed mantle. However, syn- to posteruptive atmospheric contamination for Ne, Ar, Kr, and Xe often makes it difficult to read the mantle record for these noble gases. Over the past two decades, we have been able to better resolve mantle noble gases from the pervasive syn- to posteruptive atmospheric contaminant. These new data, along with geodynamic and geochemical models, have started to shed light on major outstanding issues associated with interpreting noble gas data. The data used in this review come from continental gases that sample both the MORB (Ballentine et al. 2005, Caffee et al. 1999, Holland & Ballentine 2006, Holland et al. 2009) and plume sources (Caracausi et al. 2016) as well as basaltic glasses from mid-ocean ridges and ocean islands.

In this review, we first discuss some relevant geochemical systematics of the noble gases, their different isotopes, the production pathways for the isotopes, and the veil of syn- to posteruptive atmospheric contamination in lavas that tends to obscure the mantle composition. After establishing how mantle-derived compositions are determined, we use developments over the past two decades to discuss constraints that the noble gases place on the accretion and loss of volatiles, early differentiation, mantle structure, and the long-term evolution of the mantle.

---

**Volatiles:** used here to refer to the elements and compounds of H, C, N, S, halogens, and noble gases

**Mid-ocean ridge basalt (MORB) source:** mantle region sampled to produce MORBs over Earth's history

**Reservoir:** physical domain or region within Earth (mantle, crust, ocean, atmosphere) whose mean composition contrasts with some other domain within Earth

**Plume source:** mantle region sampled by plumes over Earth's history

---

## 2. PHYSIOCHEMICAL SYSTEMATICS OF THE NOBLE GASES

The noble gases belong to group 18 of the periodic table, and this review discusses five of the noble gases—He, Ne, Ar, Kr, and Xe. As a group, the noble gases are chemically unreactive at standard temperatures and pressures. The natural abundances and isotopic ratios of noble gases, therefore, are not influenced by biological processes or chemical reactions on Earth's surface. As a group, the noble gases behave coherently and predictably with respect to solubility, diffusivity, and crystal-melt partitioning. The solubility of the noble gases can be expressed by Henry's law,

$$C = H \times P_i,$$

where  $C$  is the dissolved concentration,  $P_i$  is the partial pressure, and  $H$  is Henry's constant, a function of pressure, temperature, and composition.

In silicate liquids, He is the most soluble while Xe is the least soluble. Equilibrium degassing of silicate liquids would therefore preferentially retain He over the heavier noble gases. During magmatic degassing, after a vapor bubble of carbon dioxide (CO<sub>2</sub>) [or dihydrogen monoxide (H<sub>2</sub>O)] forms, the noble gases partition between the silicate magma and the vapor bubble. The elemental ratios of noble gases can be predicted to change in systematic ways in the silicate liquid undergoing degassing based on the solubility of the noble gases, with heavier noble gases being preferentially lost from the magma. Deviations from this expected behavior may arise due to kinetic fractionation of the noble gases based on their different diffusivities. In silicate liquids, He appears to have the highest diffusivity and Xe the lowest (i.e., the most soluble species also diffuses the fastest). The effect of kinetic fractionation is to suppress the degree of noble gas fractionation that would be predicted based on solubility ratios: The heavier noble gases are less soluble but are unable to diffuse fast enough to attain equilibrium with the vapor bubbles. Subsequent loss of the CO<sub>2</sub> (or H<sub>2</sub>O) bubble from the magma is the mechanism by which noble gases are removed from the magma.

In water, the solubilities of the noble gases are reversed compared to silicate liquid such that Xe is the most soluble while He is the least soluble. The higher solubility of Xe in water compared to the lighter noble gases is a result of Xe being the most polarizable of the noble gases. Minerals that form in contact with seawater, or trap seawater as inclusions, tend to pick up this pattern of enrichment of heavier noble gases over the lighter noble gases (Holland & Ballentine 2006, Kendrick et al. 2011, Sumino et al. 2010). Because of the potential to recycle noble gases via subduction of seawater-derived noble gases (Holland & Ballentine 2006, Kendrick et al. 2011), the preferential solubility of the heavier noble gases in water plays an important role in setting mantle noble gas abundance patterns (Section 7).

The behavior of the noble gases during mantle melting can be expressed by the partition coefficient,  $D$ , which is the ratio of the concentration of an element in the solid to the concentration of that element in the liquid. Experiments over the past decade using advances in microanalytical techniques, such as ultraviolet (UV) laser ablation, have greatly clarified the geochemical systematics of the noble gases during partial melting (Brooker et al. 2003, Heber et al. 2007, Jackson et al. 2013). All the noble gases appear to behave as highly incompatible elements, indicating that they strongly partition into the melt rather than into silicate minerals ( $D \sim 0.001$  for Ar to  $D \leq 2 \times 10^{-4}$  for He, Ne, Kr, and Xe). Importantly, noble gases seem to be more incompatible than their radioactive parent isotopes (Section 3): He and Ne are more incompatible during partial melting than uranium (U) and thorium (Th), while Ar appears to be more incompatible than potassium (K). The highly incompatible nature of noble gases may change at very high pressures. For example, during crystallization of bridgmanite from a magma ocean under high pressures and temperatures (25 GPa, 1,800°C),  $\sim 1$  wt% of Ar might be trapped in the bridgmanite crystal lattice,

---

**Radioactive parent isotope:** unstable isotope that decays over time to transform into an isotope of a different element

---

**Primordial, or nonradiogenic, isotope:** isotope that is neither radioactive nor produced through radioactive decay; has existed in its current form since 4.5 Ga

most likely in vacancies (Shcheka & Keppler 2012). The solubilities of Kr and Xe in bridgmanite are a factor of 3 and 30 lower than Ar, respectively. Additional experiments should, however, be carried out to confirm the high pressure-temperature (P-T) behavior of noble gases relevant to conditions corresponding to crystallization of bridgmanite and ferropericlasite from a magma ocean.

### 3. NOBLE GAS ELEMENTAL AND ISOTOPIC SYSTEMATICS

The five noble gases (He, Ne, Ar, Kr, and Xe) have a diverse array of stable isotopes—23 in total (Table 1). Each of the five noble gases has at least one isotope that is stable and nonradiogenic, referred to as a primordial isotope (Table 1). Except for  $^3\text{He}$ , which continuously escapes from Earth's atmosphere to space, the present terrestrial inventory of the primordial isotopes is that acquired during Earth's accretion. Because the noble gases do not partake in biological processes and are not affected by chemical reactions, the ratio of the primordial isotopes for a given element (e.g.,  $^{20}\text{Ne}/^{22}\text{Ne}$ ) is a powerful tracer of the sources of Earth's volatiles. The ratio of primordial isotopes belonging to two different elements, sometimes referred to as an elemental ratio (e.g.,  $^3\text{He}/^{22}\text{Ne}$  or  $^3\text{He}/^{130}\text{Xe}$ ), can be affected by different physical processes, such as magmatic degassing, diffusion, or dissolution of gases into seawater. Therefore, elemental ratios such as  $^3\text{He}/^{22}\text{Ne}$ ,  $^3\text{He}/^{130}\text{Xe}$ , and  $^{22}\text{Ne}/^{36}\text{Ar}$  provide crucial information on processes that have operated on different mantle reservoirs over Earth history.

There is a zoo of noble gas isotopes produced by radioactive decay, nuclear reactions, and spontaneous fission. The radioactive parent nuclides have distinct cosmochemical behavior and span a wide range of half-lives (Table 1). For example, U and Th are refractory lithophile elements, K is a moderately volatile lithophile element, and iodine (I) is a highly volatile lithophile element that becomes siderophile at high pressures (e.g., Jackson et al. 2018). All processes that fractionate parent radionuclides from their atmophile noble gas daughters will produce radiogenic signatures

**Table 1** Noble gas isotopes

Element	Nonradiogenic (or primordial) isotopes	Radiogenic isotopes	Parent isotope	Decay mode	Half-life (Myr)
He	$^3\text{He}$	$^4\text{He}$	$^{232}\text{Th}$ $^{235}\text{U}$ , $^{238}\text{U}$	$\alpha$ $\alpha$ $\alpha$	14,001 703.8 4,468
Ne	$^{20}\text{Ne}$ , $^{22}\text{Ne}$	$^{21}\text{Ne}^{\text{a}}$	$^{232}\text{Th}$ $^{235}\text{U}$ , $^{238}\text{U}$	$^{18}\text{O}(\alpha, n)^{21}\text{Ne}$ $^{24}\text{Mg}(n, \alpha)^{21}\text{Ne}$	NA
Ar	$^{36}\text{Ar}$ , $^{38}\text{Ar}$	$^{40}\text{Ar}$	$^{40}\text{K}$	$e^-$ capture	1,251
Kr	$^{78}\text{Kr}$ , $^{80}\text{Kr}$ , $^{82}\text{Kr}$ , $^{83}\text{Kr}$ , $^{84}\text{Kr}$ , $^{86}\text{Kr}$	Minor production of $^{84}\text{Kr}$ , $^{86}\text{Kr}^{\text{c}}$	$^{244}\text{Pu}$ $^{238}\text{U}$	SF	80 4,468
Xe	$^{124}\text{Xe}$ , $^{126}\text{Xe}$ , $^{128}\text{Xe}$ , $^{130}\text{Xe}$	$^{129}\text{Xe}$ $^{131}\text{Xe}$ , $^{132}\text{Xe}$ , $^{134}\text{Xe}$ , $^{136}\text{Xe}^{\text{b,c}}$	$^{129}\text{I}$ $^{244}\text{Pu}$ $^{238}\text{U}$	$\beta^-$ SF SF	15.7 80 4,468

<sup>a</sup> $^{21}\text{Ne}$  is classified as a nucleogenic isotope as it is produced by  $\alpha$ , n or n,  $\alpha$  reactions on  $^{18}\text{O}$  and  $^{24}\text{Mg}$ , respectively. The  $\alpha$  particles are generated from decay and U and Th, and the neutrons are generated from fission of U and interaction of  $\alpha$  particles with other target nuclides (e.g., Šrámek et al. 2017).

<sup>b</sup> $^{131}\text{Xe}$ ,  $^{132}\text{Xe}$ ,  $^{134}\text{Xe}$ , and  $^{136}\text{Xe}$  are classified as fissionogenic isotopes as they are produced by spontaneous fission of  $^{244}\text{Pu}$  and  $^{238}\text{U}$ .

<sup>c</sup> $^{136}\text{Xe}$  and  $^{86}\text{Kr}$  have the highest production rates for the fission Xe and fission Kr isotopes, respectively.

The branching ratios for SF for  $^{244}\text{Pu}$  and  $^{238}\text{U}$  are  $1.25 \times 10^{-3}$  and  $5.45 \times 10^{-7}$ , respectively. The yield of  $^{136}\text{Xe}$  is 6.6 and 50 times that of  $^{86}\text{Kr}$  from  $^{238}\text{U}$  and  $^{244}\text{Pu}$  fission, respectively.

Abbreviations: Ar, argon; He, helium; I, iodine; K, potassium; Kr, krypton; Mg, magnesium; Ne, neon; NA, not applicable; O, oxygen; Pu, plutonium; SF, spontaneous fission; Th, thorium; U, uranium; Xe, xenon.

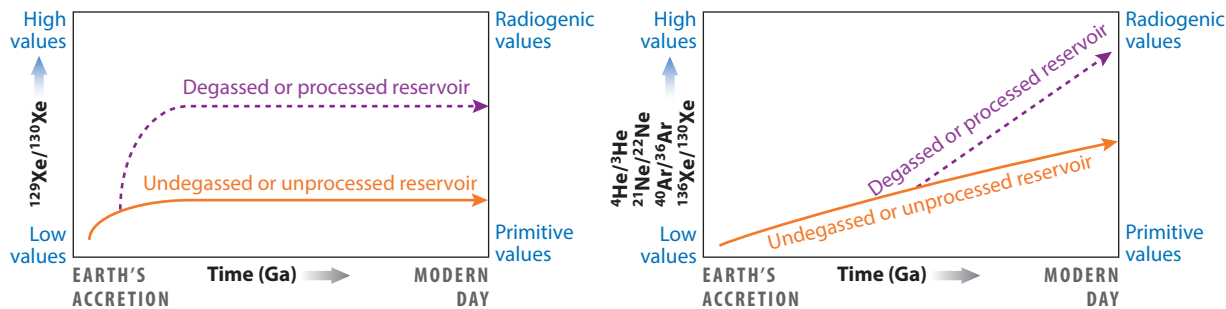


**Figure 1**

Schematic showing the time evolution of an unprocessed (undegassed) reservoir and a processed (degassed) reservoir. A processed reservoir is one that has been subject to melt extraction at a ridge or hot spot. Note that the evolution of  $^{129}\text{Xe}/^{130}\text{Xe}$  ratios stops for both the unprocessed and processed reservoir when  $^{129}\text{I}$  becomes extinct. While the schematic shows the end-member cases of an unprocessed reservoir and processed reservoir, the same relationships would map into a less-processed versus more-processed reservoir. Abbreviations: Ar, argon; He, helium; Ne, neon; Xe, xenon.

over time. As a result, the radiogenic, nucleogenic, and fissionogenic isotopes of noble gases are sensitive to timescales and processes related to Earth's accretion, core formation, formation of the Moon, degassing during the Hadean, and long-term degassing associated with plate tectonics.

The ratio of a radiogenic to primordial isotope ( $^4\text{He}/^3\text{He}$ ,  $^{21}\text{Ne}/^{22}\text{Ne}$ ,  $^{40}\text{Ar}/^{36}\text{Ar}$ ,  $^{129}\text{Xe}/^{130}\text{Xe}$ ) in a reservoir today is reflective of the time-integrated ratio of the radioactive parent to the primordial noble gas isotope. For example, the  $^4\text{He}/^3\text{He}$  ratio reflects the time-integrated  $(\text{U} + \text{Th})/^3\text{He}$  ratio, and the  $^{129}\text{Xe}/^{130}\text{Xe}$  ratio reflects the time-integrated  $\text{I}/^{130}\text{Xe}$  ratio. Since the noble gases are more incompatible than the radioactive parent isotopes, processing a mantle through partial melting generates a residual mantle reservoir with high time-integrated  $(\text{U} + \text{Th})/^3\text{He}$ ,  $(\text{U} + \text{Th})/^{22}\text{Ne}$ ,  $\text{K}/^{36}\text{Ar}$ , and  $\text{I}/^{130}\text{Xe}$  ratios. Over time, such reservoirs would evolve to more radiogenic (higher)  $^4\text{He}/^3\text{He}$ ,  $^{21}\text{Ne}/^{22}\text{Ne}$ ,  $^{40}\text{Ar}/^{36}\text{Ar}$ , and  $^{129}\text{Xe}/^{130}\text{Xe}$  ratios compared to an unprocessed reservoir (**Figure 1**). We point out that the  $^{129}\text{Xe}/^{130}\text{Xe}$  ratio is unique compared to the  $^4\text{He}/^3\text{He}$ ,  $^{21}\text{Ne}/^{22}\text{Ne}$ , or  $^{40}\text{Ar}/^{36}\text{Ar}$  ratios. That is because unlike with  $^4\text{He}$ ,  $^{21}\text{Ne}$ , and  $^{40}\text{Ar}$ , the production of  $^{129}\text{Xe}$  stops  $\sim 100$  Myr after the start of the Solar System as  $^{129}\text{I}$  becomes extinct. Consequently, variations in  $^{129}\text{Xe}/^{130}\text{Xe}$  ratios between different reservoirs could have been produced only in the first 100 Myr of Earth history (i.e., during and immediately following Earth's accretion).

Ratios of fissionogenic isotopes in mantle samples provide a robust framework for interpreting degassing timescales and processing of mantle reservoirs. Fissionogenic  $^{131}\text{Xe}$ ,  $^{132}\text{Xe}$ ,  $^{134}\text{Xe}$ , and  $^{136}\text{Xe}$  were produced from extinct plutonium ( $^{244}\text{Pu}$ ) ( $t_{1/2} = 80.0$  Myr) for the first  $\sim 500$  million years of Solar System history and continue to be produced from extant  $^{238}\text{U}$  ( $t_{1/2} = 4.468$  Gyr). Pu and U fission, however, produces the four fissionogenic Xe isotopes in distinct, characteristic proportions. A reservoir that remains completely closed to volatile loss over Earth's history has a ratio of Pu- to U-derived fissionogenic Xe ( $^{136}\text{Xe}^*_{\text{Pu}244}/^{136}\text{Xe}^*_{\text{U}238}$ ) of  $\sim 27$  (Azbel & Tolstikhin 1993, Tolstikhin & O'Nions 1996, Tolstikhin et al. 2006). In other words, the isotopic composition of the fissionogenic Xe for a closed-system reservoir would largely resemble that produced from pure  $^{244}\text{Pu}$  fission. Loss of Xe from a reservoir after  $^{244}\text{Pu}$  becomes extinct (500 Myr) would lead to a greater contribution of  $^{238}\text{U}$  fission to the fissionogenic Xe budget over time. The fraction of fissionogenic isotopes derived from  $^{244}\text{Pu}$  versus  $^{238}\text{U}$  isotopes can be obtained from the measured mantle Xe composition to infer the extent of degassing of a reservoir: the higher the fraction derived from  $^{244}\text{Pu}$ , the less degassed the reservoir.

**Radiogenic isotope:** isotope produced through radioactive decay

**Nucleogenic isotope:** isotope produced through natural nuclear reactions on Earth, such as the reaction between an  $\alpha$  particle and oxygen-18 to produce neon-21

**Fissionogenic isotope:** isotope produced through nuclear fission of radioactive isotopes

## 4. READING THE MANTLE RECORD FOR THE NOBLE GASES

**Component:** a model entity representing a conceptual homogeneous end-member composition used to describe and interpret measured compositions

Pervasive syn- to post-eruptive atmospheric contamination affects the budget of Ne, Ar, Kr, and Xe—but not He—in mantle-derived lavas. The atmospheric contamination is introduced into the samples syn- to post-eruption and is particularly severe for subaerial or shallow-submarine eruptions. In the early days of noble gas research, the syn- to post-eruptive atmospheric contamination in mantle plumes was misinterpreted as representing the composition of the lower mantle. While a few nonatmospheric  $^{40}\text{Ar}/^{36}\text{Ar}$  ratios were observed at Hawaii (e.g., Fisher 1983), the predominance of air-like compositions in mantle plumes led to models that explained the origin of the atmosphere via outgassing of the upper mantle; the lower mantle was modeled as undegassed and retained its near-atmospheric composition (e.g., Allègre et al. 1983, Sarda et al. 1988, Staudacher et al. 1986). While aspects of these models are still valid, such as deducing mantle degassing timescales from the buildup of radiogenic  $^{40}\text{Ar}$  in the atmosphere, the recognition that the mantle and the atmosphere do not have the same primordial isotopic ratios (Caffee et al. 1999, Hiyagon et al. 1992, Holland et al. 2009, Honda et al. 1991, Poreda & Farley 1992) invalidates derivation of primordial noble gases in the atmosphere from direct outgassing of the upper mantle. The above example illustrates that distinguishing syn- to post-eruption atmospheric contamination from the mantle composition in basalts is critical for using the noble gases to infer processes related to Earth's formation and evolution.

One of the most significant advances in the field of noble gas geochemistry has been to develop the analytical capability needed to look through the veil of atmospheric contamination and deduce the mantle compositions based on step-crushing (e.g., Burnard et al. 2003, Kurz et al. 2009, Moreira et al. 1998, Mukhopadhyay 2012, Parai et al. 2012, Peron et al. 2016, Petó et al. 2013) and sampling of individual bubbles through UV laser ablation in submarine and subglacial basaltic glasses (Colin et al. 2013, 2015; Peron et al. 2016, 2017; Raquin et al. 2008). Progressive crushing of basaltic glass under a vacuum ruptures different populations of bubbles trapped in the glass with varying degrees of syn- to post-eruptive contamination. As a result, in a Ne three-isotope plot ( $^{20}\text{Ne}/^{22}\text{Ne}$  versus  $^{21}\text{Ne}/^{22}\text{Ne}$ ), two-component mixing of atmospheric Ne and mantle Ne generates a suite of measured compositions that fall on a line between the mantle composition and air (**Figure 2a**). For the MORB source, the  $^{20}\text{Ne}/^{22}\text{Ne}$  ratio is established to be 12.5 (see Section 5.1). Consequently, the mantle  $^{21}\text{Ne}/^{22}\text{Ne}$  ratio can be determined by a linear regression of the data (**Figure 2a**). To determine the mantle  $^{40}\text{Ar}/^{36}\text{Ar}$  ratio, one can plot the  $^{20}\text{Ne}/^{22}\text{Ne}$  ratio of the step-crushes against the  $^{40}\text{Ar}/^{36}\text{Ar}$  ratio (**Figure 2b**). In this space, the two-component mixing is defined by a hyperbola. A hyperbolic best fit can be used to determine the mantle  $^{40}\text{Ar}/^{36}\text{Ar}$  ratio for a mantle  $^{20}\text{Ne}/^{22}\text{Ne}$  ratio of 12.5 (**Figure 2b**). Similar hyperbolic regressions can be used to determine the mantle  $^{129}\text{Xe}/^{130}\text{Xe}$  ratio, although for Xe, the best fits appear to be obtained when regressing Xe isotopic ratios against  $^{40}\text{Ar}/^{36}\text{Ar}$  ratios as the hyperbolas tend to asymptote parallel to the  $^{40}\text{Ar}/^{36}\text{Ar}$  axis (**Figure 2c**), such that a well-defined Xe isotopic ratio for the mantle can be determined without great sensitivity to the mantle  $^{40}\text{Ar}/^{36}\text{Ar}$  composition (e.g., Parai & Mukhopadhyay 2015, Parai et al. 2012, Petó et al. 2013, Tucker et al. 2012). Once one of the mantle Xe isotopic ratios is determined (e.g.,  $^{129}\text{Xe}/^{130}\text{Xe}$ ), the other Xe isotopic ratios of the mantle can be obtained by linear regression among Xe isotopes (**Figure 2d**).

After the correction for syn- to post-eruptive atmospheric contamination has been made (**Figure 2**), the noble gas isotopic ratios of the mantle can be interpreted according to partial melting processes that drive degassing and plate subduction history that drives atmosphere-derived volatiles back into the mantle. The different radioactive decay schemes with their various half-lives (**Table 1**) can be used to infer timescales for these processes, from events occurring

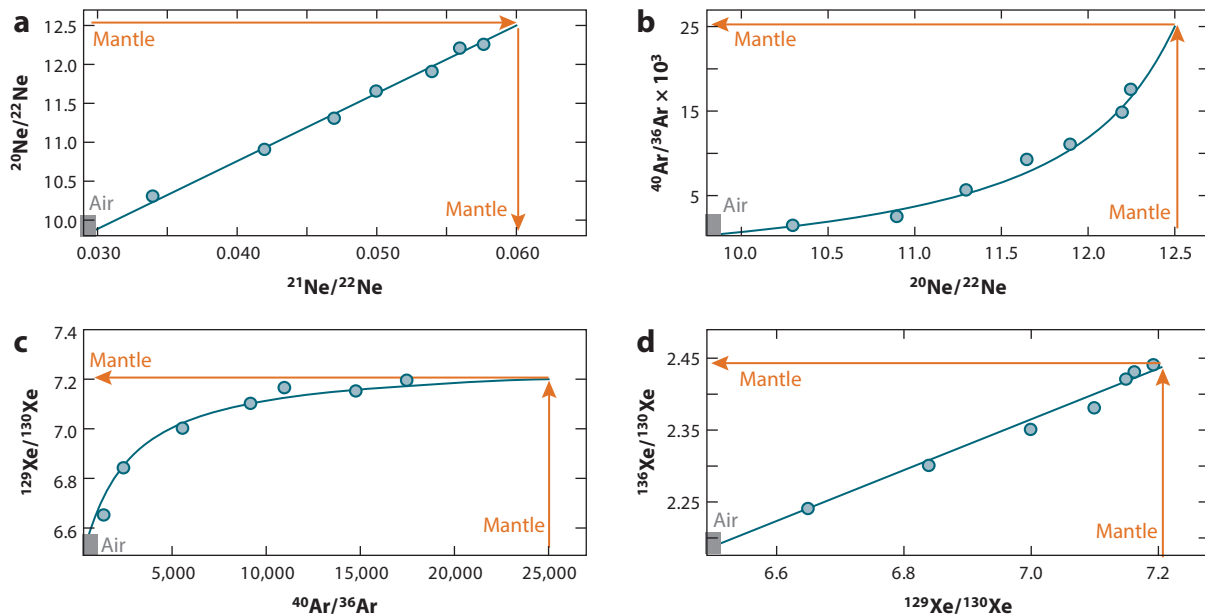


**Figure 2**

Schematic showing how step-crushing data from a basalt can be used to correct syn- to post-eruptive atmospheric contamination and determine the noble gas isotopic ratios in the mantle. In these panels, two-component mixing between air (*grey*) and the mantle (*orange*) generates bubble compositions that lie on a straight line when the same normalizing isotope is on both axes (*a,d*). Hyperbolic mixing would be expected when the normalizing isotopes on the *x*- and *y*-axes are different (*b,c*). Abbreviations: Ar, argon; Ne, neon; Xe, xenon.

during Earth's accretion, early in Earth's history (<500 Myr), continuously over Earth's history, and late in Earth's history.

The schematic shown in **Figure 2** is highly idealized. Many samples appear to have two syn- to post-eruptive atmospheric contaminants that are elementally fractionated with respect to each other. While the addition of a second syn- to post-eruptive atmospheric contaminant does not affect the linear regressions (**Figure 2a,d**) as the isotopic composition of both components appears atmospheric, the differences in elemental ratios produce significant scatter in Ne-Ar and Ar-Xe space that violates the assumption of a two-component mixing hyperbola and precludes obtaining a hyperbolic best fit (**Figure 2b,c**). As a result, only a handful of samples exist for which mantle Ar and Xe isotopic constraints are available (Moreira et al. 1998, Mukhopadhyay 2012, Parai et al. 2012, Peron et al. 2016, Pető et al. 2013, Raquin & Moreira 2009, Tucker et al. 2012). Technical advances such as bottling ocean floor dredge samples immediately upon retrieval in ultrapure nitrogen (N) may significantly reduce, or even eliminate, the syn- to post-eruptive atmospheric contamination (Mukhopadhyay et al. 2015). Using such techniques in future sample collection expeditions may allow for a much more diverse suite of samples to be characterized.

## 5. VOLATILE ACCRETION AND LOSS

Since the early 2000s, high-precision measurements of noble gases in mantle-derived basalts and in continental well gases, combined with volatile abundances in Earth's surface reservoirs, have provided new insights into the sources of terrestrial volatiles and the loss processes that have operated during Earth's accretion.

We note for the purposes of the discussion below that chondritic meteorites without significant thermal metamorphism have similar (although not identical) Ar, Kr, and Xe isotopic compositions as the Q component (Lewis et al. 1975, Wieler 1994), and Q dominates the budget of these three elements in chondrites (e.g., Ott 2014). Therefore, when referring to chondritic Ar, Kr, or Xe compositions, we refer to the average Ar, Kr, and Xe composition of chondrites. Chondritic meteorites, however, can have quite distinct  $^{20}\text{Ne}/^{22}\text{Ne}$  ratios. Only the CI chondrites appear to have a  $^{20}\text{Ne}/^{22}\text{Ne}$  ratio less than, or similar to, the terrestrial atmosphere. Other groups of chondrites show a range of compositions between CI values and solar wind irradiated values. The solar wind irradiated composition also appears in a suite of differentiated meteorites. Therefore, when referring to the solar wind irradiated meteoritic material, we refer to any meteorite with the solar wind irradiated composition.

### 5.1. Volatile Sources for the Mantle

Large differences in the primordial Ne isotopic ratio ( $^{20}\text{Ne}/^{22}\text{Ne}$ ) among potential sources of Earth's volatiles make Ne a key player in understanding the history of volatile accretion (Ballentine et al. 2005; Marty 1989; Moreira 2013; Mukhopadhyay 2012; Peron et al. 2017, 2018; Raquin & Moreira 2009; Yokochi & Marty 2004). The three potential sources of volatiles during the main phase of Earth's accretion are nebular gases, solar wind irradiated meteoritic material, and CI chondrite meteorites. The  $^{20}\text{Ne}/^{22}\text{Ne}$  ratio of nebular gas is  $13.36 \pm 0.09$  (Heber et al. 2012). In contrast, micrometer-sized dust grains irradiated by solar wind in the early Solar System and then incorporated into planetesimals would be characterized by a  $^{20}\text{Ne}/^{22}\text{Ne}$  ratio of  $\sim 12.5\text{--}12.75$  (e.g., Moreira 2013, Moreira & Charnoz 2016). Finally, CI chondrites are characterized by a  $^{20}\text{Ne}/^{22}\text{Ne}$  ratio of  $\sim 9$  (Mazor et al. 1970), significantly different from either nebular or solar wind irradiated material (Figure 3a).

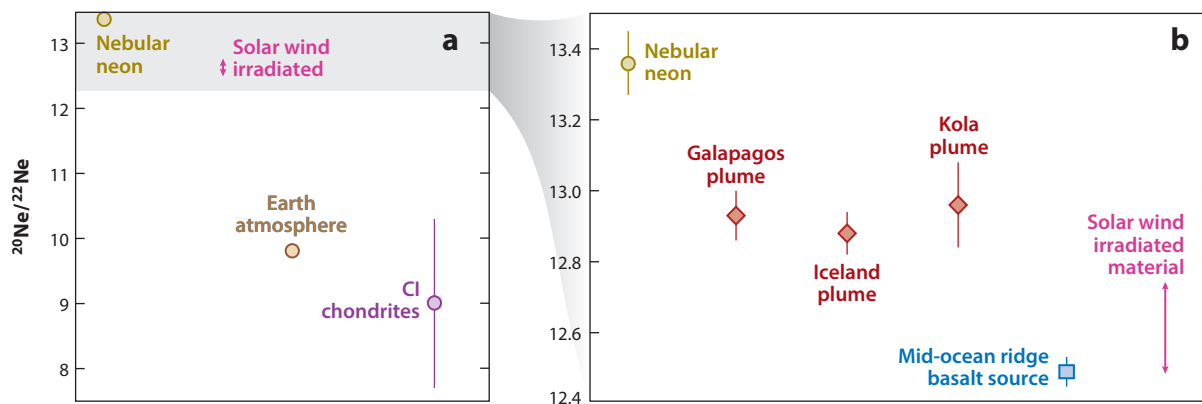


Figure 3

The Ne isotopic composition of (a) solar nebula, solar wind irradiated meteoritic material, CI chondrites, and Earth's atmosphere compared to the (b) mantle values. The nebular value is from Heber et al. (2012), the range of solar wind irradiated material is from Moreira & Charnoz (2016), and the CI chondrite data are from Mazor et al. (1970). The Galapagos, Iceland, and Kola plume points represent the highest measured values from these plumes and are from Peron et al. (2016), Mukhopadhyay (2012), and Yokochi & Marty (2004), respectively. The mid-ocean ridge basalt source is from Holland & Ballentine (2006). The large error bars for the CI chondrites reflect the inherent heterogeneity within this meteorite class rather than analytical uncertainties. Figure modeled after Schlichting & Mukhopadhyay (2018). Abbreviation: Ne, neon.

The maximum measured  $^{20}\text{Ne}/^{22}\text{Ne}$  ratios in plumes, or MORBs influenced by plumes (e.g., Iceland, the Galapagos, Kola, Discovery), appear to reach  $^{20}\text{Ne}/^{22}\text{Ne}$  values close to 12.9 (Mukhopadhyay 2012, Peron et al. 2016, Sarda et al. 2000, Yokochi & Marty 2004). This value is higher than values expected in solar wind irradiated meteoritic material and significantly higher than values in CI chondrites. Since plumes sample the deep mantle, the observation raises the intriguing possibility that within the deepest mantle there is a memory of acquisition of nebular volatiles. We use the phrase deep mantle to refer to mantle depths dominantly sampled by plumes; the region is presumably deeper than 1,000 km and close to the core-mantle boundary (CMB), but the actual depth is deliberately left vague here since the source region for plumes is still uncertain.

The potential presence of nebular volatiles in the deep mantle plume source suggests that volatile accretion started in the presence of nebular gases while Earth was an embryo. The median lifetime of a nebula is  $\sim 2.5$  Myr, although nebular gases can persist for  $\sim 10$  Myr (Wyatt 2008). The mean time of accretion for Earth is  $\sim 11$  Myr (Yin et al. 2001), while the mean accretion timescale of Mars is  $1.9^{+1.7}_{-0.8}$  Myr (Dauphas & Pourmand 2011, Tang & Dauphas 2014). The entirety of planet Earth is, therefore, unlikely to have equilibrated with the solar nebula via a global magma ocean. However, given a median lifetime of 2.5 Myr for the nebula, proto-Earth embryos (one to three times the size of Mars) could have acquired and trapped nebular volatiles in their interiors. Hence, during accretion, nebular volatiles trapped in embryo-sized bodies could have contributed to the Ne budget of Earth's deep interior that is now sampled by mantle plumes.

Except for the deep mantle plume source, signatures of nebular gases are not found elsewhere on our planet.  $^{20}\text{Ne}/^{22}\text{Ne}$  ratios in MORBs do not exceed  $\sim 12.5$  within the quoted uncertainties of the measurements (Moreira et al. 1998, Parai et al. 2012, Peron et al. 2017, Raquin & Moreira 2009, Sarda et al. 2000, Tucker et al. 2012), which are similar to values of meteoritic material irradiated by the solar wind (e.g., Peron et al. 2017, 2018). The maximum measured MORB values are similar to an independent estimate of  $12.49 \pm 0.04$  for the MORB source based on continental well gases (Ballentine et al. 2005, Holland & Ballentine 2006). These well gases represent a three-component mixture: Crustal fluids are contaminated with air, and upper mantle fluids are variably added to this mixed shallow contaminant as they percolate through the crust. The mixing line displayed by the continental well gases is, therefore, steeper than the MORB-air mixing line and intersects the MORB-air mixing line. The intersection point was suggested to define the composition of the MORB mantle at a  $^{20}\text{Ne}/^{22}\text{Ne}$  ratio of  $12.49 \pm 0.04$  (Ballentine et al. 2005, Holland & Ballentine 2006). Ne in the MORB source could therefore be derived from solar wind irradiated meteoritic material, from a mixture of nebular and atmospheric Ne, or from a mixture of nebular and CI chondritic material (e.g., Kendrick et al. 2011) (**Figure 3**).

The primordial isotopic ratio of Ar ( $^{38}\text{Ar}/^{36}\text{Ar}$ ) in both plumes and MORBs is similar to chondritic values (Mukhopadhyay 2012; Peron et al. 2016, 2017; Raquin & Moreira 2009). Recent high-precision measurements reveal that the primordial Xe isotopic ratios (e.g.,  $^{124}\text{Xe}/^{130}\text{Xe}$ ) of plumes (Caracausi et al. 2016) and the primordial Kr isotopic ratios of the MORB source (e.g.,  $^{84}\text{Kr}/^{82}\text{Kr}$ ) are chondritic (Holland et al. 2009). Furthermore, even the deep mantle  $^{20}\text{Ne}/^{22}\text{Ne}$  values are not identical to nebular values (**Figure 3b**), and Earth's major volatiles [hydrogen (H), carbon (C), and N] are chondritic in composition (Alexander 2017; Alexander et al. 2012, 2017; Marty 2012). Taken together, these observations suggest that most of the nebular volatiles acquired by the proto-Earth embryo were lost and replaced with later-accreted volatiles. The loss of nebular volatiles from within Earth, during the embryo stage, may be a necessary consequence of the accretion history of Earth. After the nebula dissipates, the proto-Earth grows through accretion of planetesimals and through giant impacts associated with collisions between embryos. Since magma oceans are a consequence of giant impacts, the collisions between embryos should have released a large fraction of nebular gases trapped within the solid Earth into a transient

atmosphere. Hydrodynamic escape of this atmosphere and/or subsequent impacts could have led to loss of these nebular volatiles from the Earth embryo. Alternatively, some of the nebular volatile elements may have been sequestered in the core. Since a solidified and degassed magma ocean would be severely depleted in heavy noble gases (they are least soluble in a magma ocean), later-accreted chondritic materials enriched in the heavy noble gases might dominate the final deep Earth budgets of these elements without overprinting the light noble gas isotopic signatures.

## 5.2. Timing of Accretion of Chondritic Volatiles

Following the loss of nebular gases, the volatile inventory in the mantle was most likely replenished through delivery of chondritic volatiles after the dissipation of the nebula. The timing of acquisition of chondritic volatiles is currently a subject of debate (e.g., Halliday 2013, Hirschmann 2016, Marty 2012, Tucker & Mukhopadhyay 2014). Two possible hypotheses are that (a) the majority of these volatiles were delivered before the Moon-forming giant impact and (b) volatiles were delivered associated with late accretion, where late accretion is defined as the last 0.3–1% of Earth's mass that was accreted after the core was chemically isolated, which is assumed to be shortly after the formation of the Moon (Dauphas & Morbidelli 2014, Morbidelli & Wood 2015). We next discuss when this addition of chondritic volatiles to Earth's mantle could have occurred.

The relative abundances of the major volatile elements, as well as the isotopic ratios of the noble gases, provide key insights into when chondritic volatiles were delivered. For example, while the N and H isotopic ratios of bulk silicate Earth are chondritic, the N/H ratio (**Figure 4**) does not match any known Solar System object (Halliday 2013). The low N/H ratio of Earth presents a challenge to models where chondritic volatile elements are entirely acquired in association with late accretion: If this were the case, the terrestrial N/H ratio would not be fractionated relative to chondrites. Halliday (2013) concluded that water was delivered during the main phase of accretion. Halliday (2013) calculated that if the entire N budget was delivered during late accretion, then ~70% of Earth's H, in the form of water, was delivered before the Moon-forming impact and retained preferentially relative to N in order to account for the low N/H ratio of Earth compared

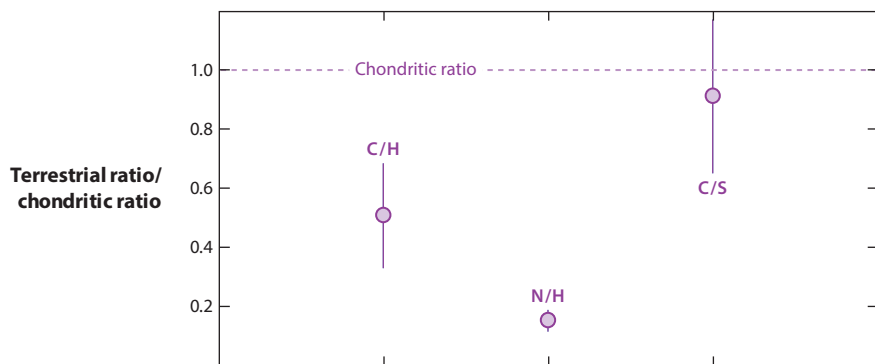


**Figure 4**

Terrestrial abundances of C/H, N/H, and C/S relative to chondritic ratios. These abundance patterns help to interpret the information recorded by the noble gases. Likewise, the noble gas isotopic and elemental abundance patterns help to inform what processes could have given rise to bulk silicate Earth volatile elemental patterns distinct from those found in chondrites. H, C, and N data are from Marty (2012) and Halliday (2013). Figure adapted from Tucker & Mukhopadhyay (2014). Abbreviations: C, carbon; H, hydrogen; N, nitrogen; S, sulfur.

to chondrites. Alternatively, Tucker & Mukhopadhyay (2014) argued that the low terrestrial C/H and N/H ratios (**Figure 4**) reflect modification of the chondritic elemental abundance patterns through loss of the more atmophile element N associated with atmospheric loss from Earth. Loss of the atmosphere, which would also lead to loss of noble gases from Earth, could be driven by giant impacts (e.g., Tucker & Mukhopadhyay 2014) or impacts of planetesimals that are more effective in eroding the atmosphere than giant impacts (Schlichting & Mukhopadhyay 2018, Schlichting et al. 2015). In this scenario, the major volatiles and mantle noble gases are residual to volatile losses that happened during the main phase of Earth's accretion.

Hirschmann (2016) argued that most of Earth's water was delivered before the Moon-forming giant impact but that late accreting materials added C and sulfur (S) to the Earth's mantle and surface reservoirs after the formation of the Moon. Both C and S are expected to strongly partition into Earth's core, although C is more siderophile than S. Hence, core formation should have left silicate Earth with a low C/S ratio compared to chondrites. However the C/S ratio of the silicate Earth is chondritic, suggesting significant C and S replenishment happened after cessation of core formation. Hirschmann's (2016) argument about significant volatile delivery after the formation of the Moon, while compatible with some aspects of noble gas geochemistry, also presents a challenge. We argue below that the primordial noble gases in the atmosphere were derived after the formation of the Moon, but the chondritic noble gases (e.g., Kr and Xe) in Earth's interior were derived before the formation of the Moon.

Inferences about the relative timing of accretion of mantle and atmospheric noble gases can be drawn based on Kr and Xe isotopes. For example, while the mantle Kr and Xe isotopic compositions are chondritic, atmospheric Kr and Xe are not chondritic (**Figure 5**). Compared to the atmosphere, the mantle is depleted in the lighter isotopes of Kr but enriched in the lighter isotopes of Xe (Holland et al. 2009) (**Figure 5**). This observation demonstrates that the atmospheric Kr and Xe isotopic compositions cannot be explained by mantle outgassing by itself, or by mantle outgassing combined with a mass fractionating loss process, such as hydrodynamic escape (**Figure 5**). The atmosphere also contains >90% of the budget of Kr and Xe in the bulk silicate Earth (Halliday 2013, Marty 2012). The differences in isotopic composition (**Figures 3 and 5**) along with the distribution of the total terrestrial budget of the noble gases between the atmosphere and the solid Earth indicate that the present-day inventory of primordial noble gases in the atmosphere was largely derived after the last major equilibration of Earth's surface reservoirs with the interior—that is, after the giant impact that formed the Moon. Therefore, the chondritic inventory of mantle noble gases was likely established before, or in association with, the Moon-forming giant impact.

Delivery of the entire atmospheric budget of noble gases via CI chondritic planetesimals during late accretion is, however, a challenging proposition to satisfy. First, the isotopic composition of Xe in the atmosphere cannot be derived from a known chondritic source (e.g., Pepin 1991). Second, if late accreting material had a CI chondrite composition, then the late accreting material composed ~4.5% of Earth's mass to satisfy the Kr budget (Marty 2012), a number that would lead to significant overabundances in the terrestrial budget of platinum group elements. Delivery of a small amount of comets has been invoked to resolve this (Halliday 2013; Marty et al. 2016, 2017). Laboratory experiments (Bar-Nun et al. 2007, Notesco et al. 2003) and recent measurements of comets (Altwegg et al. 2015; Marty et al. 2016, 2017) suggest that cometary ices can trap significant amounts of noble gases. Furthermore, the Xe isotopic composition of comets may be a suitable isotopic precursor of atmospheric Xe (Marty et al. 2017). If the laboratory experiments and cometary measurements are representative of protoplanetary ices, then the atmospheric noble gas budget could have been delivered by cometary ices representing ~0.1% of the total late accretion mass. While the H and N isotopic compositions of comets can be significantly heavier

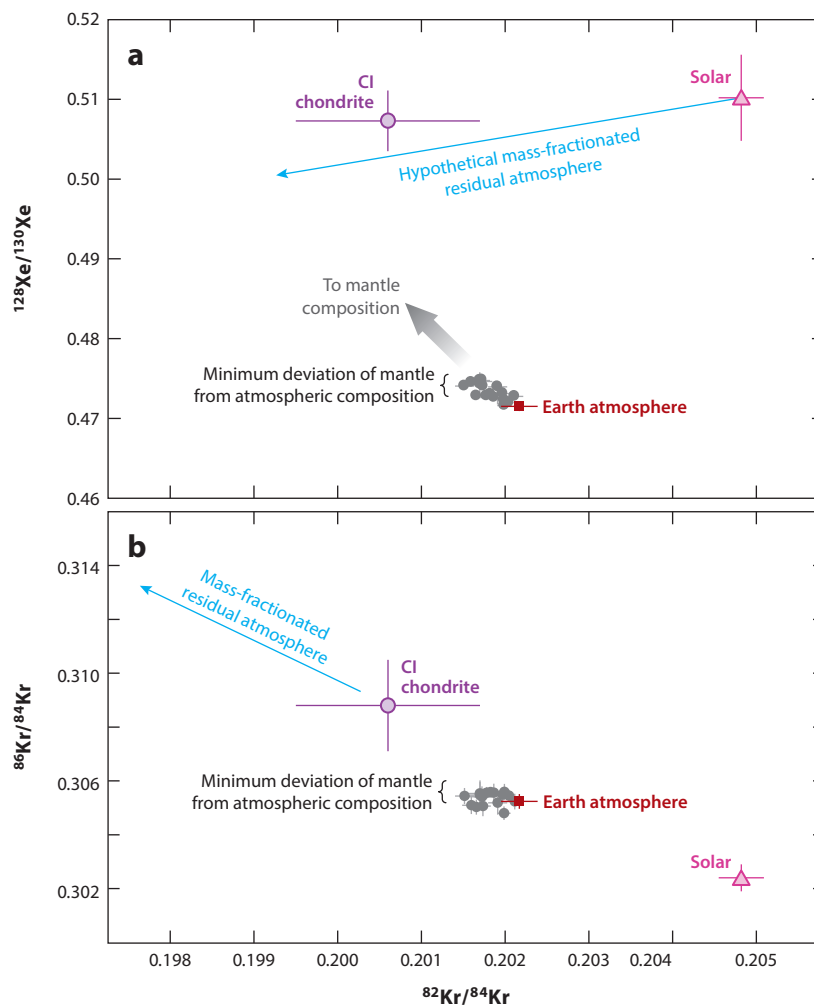


**Figure 5**

(a)  $^{128}\text{Xe}/^{130}\text{Xe}$  versus  $^{82}\text{Kr}/^{84}\text{Kr}$  and (b)  $^{86}\text{Kr}/^{84}\text{Kr}$  versus  $^{82}\text{Kr}/^{84}\text{Kr}$  for the mantle-derived  $\text{CO}_2$  natural gas from Bravo Dome, New Mexico, USA. The measurements have not been corrected for syn- to posteruptive atmospheric contamination. Therefore, the measured excesses reflect the minimum enrichment of the heavier Kr isotope ( $^{84}\text{Kr}$ ) and lighter Xe isotope ( $^{128}\text{Xe}$ ) in the mantle source of the  $\text{CO}_2$  natural gases. Also shown for reference are Earth atmosphere, solar, and CI chondrite compositions as well as the isotopic evolution of a residual atmosphere as a progressively greater amount of an initially solar atmosphere is lost. Starting with a solar or chondritic composition, producing the atmospheric  $^{128}\text{Xe}/^{130}\text{Xe}$  ratio through hydrodynamic escape would lead to a much larger  $^{82}\text{Kr}/^{84}\text{Kr}$  fractionation than observed in air. Since the mantle source of the  $\text{CO}_2$  natural gases has a lower  $^{82}\text{Kr}/^{84}\text{Kr}$  than air, adding outgassed Kr from this reservoir to the mass fractionated atmosphere cannot produce the present-day atmospheric Kr composition (Holland et al. 2009). Data are from Holland et al. (2009). Abbreviations:  $\text{CO}_2$ , carbon dioxide; Kr, krypton; Xe, xenon.

than chondritic sources (e.g., Bockelée-Morvan et al. 1998, Jehin et al. 2009, Manfroid et al. 2009, Meech et al. 2009, Meier et al. 1998), accretion of such a small amount of cometary ice would lead to no detectable change in the H or N budget of Earth. Therefore, the isotopic composition of these major volatile elements would not be perturbed away from chondritic values, whereas atmospheric noble gas isotopes would be influenced by cometary ice (Halliday 2013; Marty et al. 2016, 2017).

In summary, the noble gases suggest a complex story of volatile inheritance, loss, and replenishment. Importantly, the present-day budgets of the different volatile elements appear to be sensitive to different stages of accretion. Volatile element budgets are governed by the balance between their abundances in various accreting materials and their loss to outer space by erosion of an atmosphere (Tucker & Mukhopadhyay 2014) or loss to the core. Acquisition of volatile elements started in the embryo stage, evidence for which survives in the primordial Ne isotopic composition of plumes. With the dissipation of the nebula, planetary growth enters the giant impact phase of accretion—a stage marked by addition of major volatiles with chondritic composition and volatile loss from the silicate portion of the growing Earth to space or to the core. During this stage, water and most likely all the volatile elements were partially retained. After the Moon-forming giant impact, atmospheric noble gases were replenished by late accreting material. The bulk of the atmospheric noble gas budget was likely derived from accretion of  $\sim 2 \times 10^{22}$  g of icy planetesimals, constituting a minor portion (0.1%) of the late accretion mass (Marty et al. 2016), although addition of a small amount of chondritic noble gases to the atmosphere cannot be ruled out. The delivery of icy planetesimals could have occurred during the main phase of late accretion or at the very tail end of late accretion (e.g., Marty et al. 2016).

### 5.3. Volatile Loss Processes

The noble gases provide critical clues regarding volatile loss processes that could have occurred during Earth's accretion (Marty 2012, Moreira 2013, Tucker & Mukhopadhyay 2014). As discussed in Section 5.1, there is evidence from mantle plumes that nebular gases were acquired and retained in the deep mantle, but signatures of nebular gases are not seen in the shallower MORB source or in the atmosphere. This observation suggests loss of nebular volatiles during Earth's accretion. A simple calculation can be done based on the radiogenic Xe budget to show significant volatile loss during accretion. The abundance of  $^{127}\text{I}$  in the bulk silicate Earth is 5–10 ppb (Avice & Marty 2014, Lodders & Fegley 1998). With an initial  $^{129}\text{I}/^{127}\text{I}$  ratio of  $1.0 \times 10^{-4}$  (Ozima & Podosek 2002), the decay of  $^{129}\text{I}$  to  $^{129}\text{Xe}$  should have produced  $\sim 1.5\text{--}3 \times 10^{13}$  mol of radiogenic  $^{129}\text{Xe}$  on Earth. The atmospheric abundance of radiogenic  $^{129}\text{Xe}$  is  $\sim 2.8 \times 10^{11}$  mol (Pepin 1991). The mantle budget is uncertain but is lower than the Xe budget of the atmosphere (Pepin & Porcelli 2002). Thus,  $>97\%$  of the expected budget of radiogenic  $^{129}\text{Xe}$  has been lost from Earth. While Xe appears to have been lost from Earth's atmosphere to space during the Hadean and Archean (e.g., Avice et al. 2017, Pujol et al. 2011), this loss process by itself is not enough to account for the entire budget of radiogenic  $^{129}\text{Xe}$  lost. Accounting for the Xe loss that occurred in the Archean, Avice & Marty (2014) showed that  $\sim 75\%$  of radiogenic  $^{129}\text{Xe}$  was lost before  $\sim 60$  Ma, likely during the giant impact phase of accretion. The significant loss of radiogenic  $^{129}\text{Xe}$  before or during the giant impact phase of accretion should not be taken to imply that all the major volatiles were also extensively lost and then largely replenished after the Moon-forming giant impact, as major volatiles may have been apportioned between the growing Earth and its atmosphere differently from Xe.

Hydrodynamic escape has been invoked to explain the loss of volatiles, including Xe, from Earth's atmosphere (Dauphas 2003, Pepin 1991, Pepin & Porcelli 2006). Hydrodynamic loss,

however, requires an H-rich atmosphere, such as would be present if a nebular atmosphere were captured by the proto-Earth. In fact, models for hydrodynamic escape start off with a solar composition gas and explain present-day atmospheric volatile abundances through loss of the H<sub>2</sub>-rich atmosphere followed by resupply from the mantle and delivery of planetesimals during the late accretion (Dauphas 2003, Pepin 1991).

The present-day terrestrial volatile element signature, however, shows no evidence of hydrodynamic escape. Hydrodynamic escape fractionates isotopes of a given species as the escaping H<sub>2</sub> preferentially drags lighter isotopes to space, leaving the residual atmosphere enriched in heavier isotopes. Therefore, the present-day chondritic isotopic compositions of H, C, N, and chlorine (Cl) (Alexander et al. 2012, 2017; Marty 2012; Sharp & Draper 2013) would require the H<sub>2</sub> flux to space to fortuitously cease exactly at the point when chondritic isotopic compositions are reached. Importantly, because the mass differences between the isotopes are different for the different elements, escape for the different volatile elements would have to stop at different times—each cut-off being precisely at the point when chondritic isotopic compositions were achieved for a given volatile element. Such a scenario requires extreme fine-tuning of the H<sub>2</sub> escape flux and appears highly implausible. An alternate scenario was proposed in which the present-day isotopic compositions of the noble gases in the atmosphere were the result of adding isotopically light volatiles sequestered in the mantle to the isotopically heavy residual atmosphere produced through hydrodynamic escape (Pepin 1991; Pepin & Porcelli 2002). However, isotopic measurements indicate that the mantle is actually enriched in heavy Kr isotopes compared to the atmosphere (Holland et al. 2009). Therefore, hydrodynamic escape cannot be the primary loss mechanism that generated the signature recorded in the present-day terrestrial volatile budget. The lack of evidence for hydrodynamic escape in the present-day terrestrial volatile signatures does not imply that hydrodynamic escape never occurred. Hydrodynamic escape may have taken place on embryos shortly after the nebular gas dissipated (e.g., Erkaev et al. 2014). For our present-day planet, it appears that if hydrodynamic escape occurred early in the accretion history (i.e., during the embryo stage), the resulting chemical signature has been completely overprinted by volatile resupply and additional loss mechanisms that did not fractionate isotopic compositions.

A process capable of driving volatile loss without isotopic fractionation is bulk ejection of the atmosphere driven by giant impacts and impacts of planetesimals (Genda & Abe 2005, Schlichting et al. 2015). Atmospheric erosion associated with planetesimals has recently been shown to be quite efficient (Schlichting et al. 2015). While impact-driven loss does not fractionate isotopic compositions as it involves bulk ejection of the atmosphere, impact-driven losses can fractionate the abundance patterns of volatile elements. This is because during impacts, water oceans and crust would be retained preferentially compared to the atmosphere. Thus, elements residing in the atmosphere (N, noble gases) would be lost in preference to those in the ocean and crust (H and C) (**Figure 4**).

Dynamic simulations of terrestrial planet formation suggest that multiple giant impacts grew planets like Earth (Jacobson & Morbidelli 2014, O'Brien et al. 2006, Walsh et al. 2011). The Moon-forming giant impact was the last giant impact and corresponded with the end of core formation. The record of noble gas delivery and loss from the mantle and atmosphere discussed so far should therefore be interpreted according to multiple accretion and loss events. Overall, the noble gases paint a picture of the origins of Earth's volatile budget: The noble gases record both heterogeneous volatile delivery (Sections 5.1 and 5.2) and violent loss processes during accretion. While late accretion contributed volatiles to Earth (e.g., Albarède 2009, Hirschmann 2016, Marty 2012), it did not completely overprint the signatures of volatile accretion and loss from the main stage of Earth's accretion (Dauphas & Morbidelli 2014, Halliday 2013, Tucker & Mukhopadhyay 2014).

## 6. PRESERVATION OF SIGNATURES ASSOCIATED WITH EARLY DIFFERENTIATION AND VOLATILE LOSS PROCESSES IN THE MODERN-DAY MANTLE

During Earth's formation, accretion and loss of volatiles occurred in association with violent events that partially or completely melted the growing planet. These events led to differentiation of Earth and have left their mark in the present-day geochemistry of the mantle.

### 6.1. Magma Ocean Signatures

In the present-day mantle,  $^3\text{He}/^{22}\text{Ne}$  ratios span a large range from  $\sim 2$  to  $\geq 10$  (Coltice et al. 2011, Peron et al. 2016, Raquin & Moreira 2009, Tucker & Mukhopadhyay 2014) (**Figure 6**). Plumes that exhibit noble gas isotope signatures suggesting minimal processing by partial melting, such as the Galapagos and Iceland, have  $^3\text{He}/^{22}\text{Ne}$  ratios of 2–3 (Kurz et al. 2009, Mukhopadhyay 2012, Raquin & Moreira 2009), while average MORB has a  $^3\text{He}/^{22}\text{Ne}$  ratio of  $6.6 \pm 1$  (Tucker et al. 2018) and depleted MORB has a ratio of  $\geq 10$ .  $^3\text{He}/^{22}\text{Ne}$  values intermediate between plumes and depleted MORBs were interpreted to be due to mixing between the MORB source and the plume source by Tucker & Mukhopadhyay (2014). The primitive reservoir sampled by plumes has a higher  $^3\text{He}/^{22}\text{Ne}$  ratio than potential precursor compositions by at least a factor of 1.5 (**Figure 6**). The  $^3\text{He}/^{22}\text{Ne}$  ratio in average MORBs is higher than in potential volatile sources by at least a factor of 4.5, and the  $^3\text{He}/^{22}\text{Ne}$  ratio in depleted MORBs is higher by at least a factor of 6 (**Figure 6**). Thus, mantle reservoirs are strikingly characterized by a  $^3\text{He}/^{22}\text{Ne}$  ratio higher than even that of the Sun (**Figure 6**). Since Earth's interior is highly unlikely to be enriched in  $^3\text{He}$  compared to the Sun, the more likely scenario is that the mantle has preferentially lost  $^{22}\text{Ne}$ .

The solubility of He in a basaltic liquid is twice as high as the solubility of Ne. Honda & McDougall (1998) argued that magma ocean outgassing increased the MORB source  $^3\text{He}/^{22}\text{Ne}$  ratio relative to potential precursor compositions, as degassing would preferentially release Ne

**Primitive reservoir:** reservoir formed during Earth's accretion that is relatively unprocessed but incorporates some recycled material

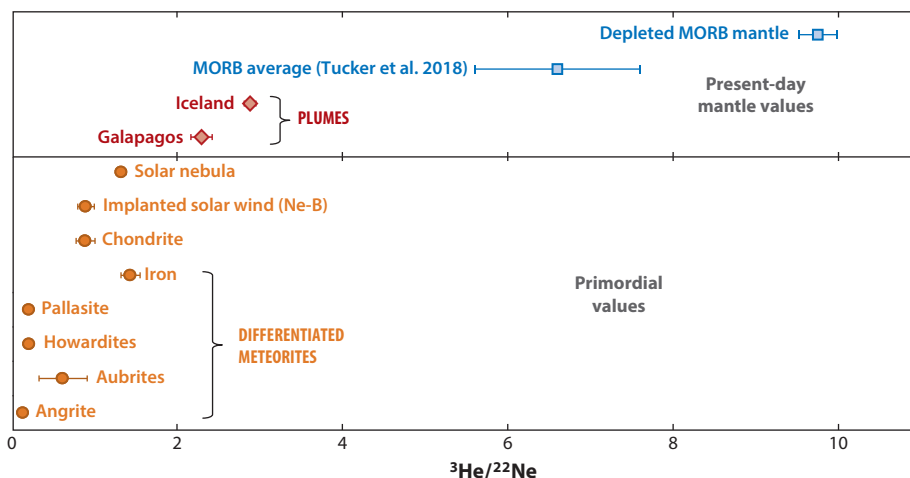


**Figure 6**

$^3\text{He}/^{22}\text{Ne}$  ratios in modern terrestrial reservoirs along with  $^3\text{He}/^{22}\text{Ne}$  ratios in possible sources that may have contributed primordial He and Ne to Earth. Figure after Tucker & Mukhopadhyay (2014), with the average MORB value from Tucker et al. (2018) and solar nebula value from Heber et al. (2012).

Abbreviations: B, boron; He, helium; MORB, mid-ocean ridge basalt; NE, neon.

over He into the atmosphere. They also noted that the lower  $^3\text{He}/^{22}\text{Ne}$  ratio of plumes might indicate a less-degassed source that was largely isolated from the MORB source for most of Earth's history.

More recently, the  $^3\text{He}/^{22}\text{Ne}$  ratio of plumes was interpreted as the signature of a basal magma ocean (BMO) (Coltice et al. 2011, Moreira 2013). A global magma ocean likely existed in the aftermath of the Moon-forming giant impact. As the magma ocean cooled, the peridotite liquidus would have intersected the isentrope in the mid-lower mantle (e.g., Mosenfelder et al. 2009, Thomas et al. 2012). Thus, instead of crystallization commencing at the CMB, crystallization would have begun at mid-mantle depths and would ultimately have isolated a layer of molten mantle above the CMB—the BMO (Labrosse et al. 2007). Incompatible elements, such as the noble gases, would be concentrated in the liquid as crystallization proceeded in the BMO. Late-crystallizing minerals could have relatively high noble gas concentrations and low  $^3\text{He}/^{22}\text{Ne}$  ratios if both He-Ne partition coefficients are on order 0.01 at high pressure (Coltice et al. 2011). Since iron (Fe) becomes enriched in the residual liquid as the BMO crystallizes, late-crystallizing minerals would be Fe enriched and likely denser than the surrounding mantle assemblage. Given its high density, the low  $^3\text{He}/^{22}\text{Ne}$  reservoir would be entrained to low degrees in convective flow, preserving the reservoir over the age of Earth. Coltice et al. (2011) noted that the factor of 5–10 times higher  $^3\text{He}/^{22}\text{Ne}$  value in MORBs was not explained by their model and could reflect mantle degassing, although they did not specify when or how this degassing occurs.

To explain the low  $^3\text{He}/^{22}\text{Ne}$  ratios and solar-like  $^{20}\text{Ne}/^{22}\text{Ne}$  ratios of  $\geq 12.9$  in plumes, Tucker & Mukhopadhyay (2014) proposed ingassing of nebular gas from a gravitationally accreted nebular atmosphere into a magma ocean, a hypothesis previously proposed based on He abundances and Ne isotopes (Harper & Jacobsen 1996, Mizuno et al. 1980, Mukhopadhyay 2012, Porcelli et al. 2001, Sharp 2017, Yokochi & Marty 2004). Ingassing of nebular gases into a magma ocean would raise the  $^3\text{He}/^{22}\text{Ne}$  ratio of the magma ocean from the nebular value of 1.5 to values of  $\sim 2$ –3 because of the He/Ne solubility ratio of  $\sim 2$  in the magma ocean. Magma ocean ingassing most likely occurs during the embryo stage. Following loss of the nebular atmosphere, and during the giant impact phase of terrestrial growth, at least two separate magma ocean degassing episodes raised the  $^3\text{He}/^{22}\text{Ne}$  ratio of the shallower mantle from  $\sim 2$ –3 to 6–10, with the last magma ocean associated with the Moon-forming giant impact (**Figure 6**). During the giant impact phase, the low  $^3\text{He}/^{22}\text{Ne}$  ratio of the deep mantle must have been preserved. Thus, Tucker & Mukhopadhyay (2014) argued that the later giant impacts, including the Moon-forming giant impact, may not have produced a whole mantle magma ocean because the timescale for turnover of a turbulently convecting magma ocean may be as short as a few weeks (Elkins-Tanton 2008, Pahlevan & Stevenson 2007, Solomatov 2000) and the magma ocean would be expected to be chemically homogeneous. However, if a dense basal layer existed before the generation of the magma ocean, a whole mantle magma ocean may not be homogenized, as the dense liquid layer would resist mixing with the rest of the magma ocean (Nakajima & Stevenson 2015). The generation of multiple magma oceans suggested by the  $^3\text{He}/^{22}\text{Ne}$  ratio is compatible with dynamic simulations that suggest multiple giant impacts during Earth's accretion (e.g., Jacobson et al. 2014).

## 6.2. Xenon Isotopes: Tracking Ancient Reservoirs

In addition to characteristically low  $^3\text{He}/^{22}\text{Ne}$  ratios, plumes are characterized by less radiogenic  $^4\text{He}/^3\text{He}$ ,  $^{21}\text{Ne}/^{22}\text{Ne}$ ,  $^{40}\text{Ar}/^{36}\text{Ar}$ , and  $^{129}\text{Xe}/^{130}\text{Xe}$  ratios compared to MORBs (**Figure 1**). In particular, low  $^4\text{He}/^3\text{He}$  ratios in plumes have been the cornerstone of models that have invoked convective isolation of the plume source. In early models, the entire lower mantle (i.e., the mantle below the transition zone) was often invoked as the source of mantle plumes (e.g.,

Allègre et al. 1987, Porcelli & Wasserburg 1995). However, a convectively isolated lower mantle is not compatible with observations of slab subduction into the lower mantle (Kárason & Van Der Hilst 2000). More recently, domains delineated by seismology, such as the D' layer (Tolstikhin & Hofmann 2005) or large low-shear wave velocity provinces (Jackson & Carlson 2011) within the lower mantle, have been advocated as the potential reservoirs hosting low (primitive)  $^4\text{He}/^3\text{He}$  ratios. There are also several alternative interpretations that assign primitive  $^4\text{He}/^3\text{He}$  ratios to discrete blobs of viscous material passively advected in the ambient mantle (Becker et al. 1999), to diffusion of  $^3\text{He}$  from the outer core into the mantle's lower thermal boundary layer (Bouhifd et al. 2013, Jephcoat 1998), to isolation of the plume source from the MORB source for  $>1$  Gyr (Class & Goldstein 2005), or to a plume source that has been less processed by partial melting relative to the MORB source (Gonnermann & Mukhopadhyay 2009).

A key reason a multitude of interpretations exist to explain low  $^4\text{He}/^3\text{He}$  ratios in plumes is that the He isotopic ratio evolves continuously over Earth's history as U and Th are extant radioactive elements (**Table 1**). Accordingly, He isotopic differences between plumes and MORBs do not have to reflect processes tied to Earth's accretion or its early differentiation. Rather, these differences could have been generated by a plate tectonic process over Earth's history via any one of numerous proposed mechanisms (discussed further in Section 7).

Mantle Xe isotopic ratios provide powerful tools to investigate degassing and mantle processing that occurred both early in Earth's history and over billion-year timescales (**Table 1**); Xe isotopic compositions of the mantle can thus be used to refine our understanding of when differences between plume and MORB reservoirs were established. In particular, the  $^{129}\text{Xe}/^{130}\text{Xe}$  ratio is uniquely suited to provide insights into early Earth processes.  $^{129}\text{I}$ , which  $\beta$  decays to  $^{129}\text{Xe}$ , becomes extinct  $\sim 100$  Myr after the start of the Solar System. Therefore, variations in  $^{129}\text{Xe}/^{130}\text{Xe}$  ratios can be produced only during the first 100 Myr of Solar System history.

While differences in measured Xe isotopic compositions between MORBs and plumes have long been recognized (Harrison et al. 1999, Hennecke & Manuel 1975, Kaneoka & Takaoka 1978, Poreda & Farley 1992, Trieloff et al. 2000), the interpretation of the isotopic differences remained unclear until recently. In general,  $^{129}\text{Xe}/^{130}\text{Xe}$  ratios in plumes are lower than MORBs, with the highest values reaching 6.8 to 7.0, compared to MORB values of 7.8 to 7.9 (Holland & Ballentine 2006, Kunz et al. 1998, Moreira et al. 1998, Mukhopadhyay 2012, Parai et al. 2012, Petó et al. 2013, Poreda & Farley 1992, Sarda et al. 2000, Staudacher & Allègre 1982, Trieloff et al. 2002, Tucker et al. 2012). Since the atmospheric  $^{129}\text{Xe}/^{130}\text{Xe}$  ratio of 6.49 is lower than the measured plume compositions, the differences between plume and MORB lavas could reflect any combination of three processes: (a) a higher degree of syn- to posteruptive atmospheric contamination of plume lavas, (b) mixing between subducted atmospheric Xe and MORB Xe (Holland & Ballentine 2006, Poreda & Farley 1992, Trieloff & Kunz 2005), or (c) different I/Xe ratios for the plume and MORB sources (Allègre et al. 1987, Poreda & Farley 1992).

High-precision Xe isotopic data in a basalt sample from the Iceland plume and a sample from the Rochambeau Rift, which samples the Samoan plume, demonstrate that models (a) and (b) above fail to explain the differences in  $^{129}\text{Xe}/^{130}\text{Xe}$  ratios between MORBs and plumes. These reflect distinct I/Xe ratios for the two sources during the lifetime of  $^{129}\text{I}$  (Mukhopadhyay 2012, Petó et al. 2013) (**Figure 7**). The Iceland, Rochambeau, and MORB sources, along with the atmospheric composition, are plotted in  $^{129}\text{Xe}/^{130}\text{Xe}-^3\text{He}/^{130}\text{Xe}$  space (**Figure 7**). Two-component mixing in this space is linear. Since the MORB and plume source compositions are not colinear with the atmospheric composition, adding subducted air or a shallow-level air contaminant to a MORB source cannot produce the lower  $^{129}\text{Xe}/^{130}\text{Xe}$  ratios in plumes. Consequently, the plume source as sampled at Iceland and Rochambeau evolved with a different I/Xe ratio than the MORB source, and the two mantle sources started differentiating before 4.45 Ga. The signature of this

---

#### Primitive $^4\text{He}/^3\text{He}$ ratio:

ratio of radiogenic- $^4\text{He}$  to primordial- $^3\text{He}$  that over 4.5 Ga has evolved significantly less than that in the degassed MORB reservoir

#### Mantle processing:

extraction of partial melts from a mantle reservoir, leading to depletion of incompatible elements in that reservoir

---

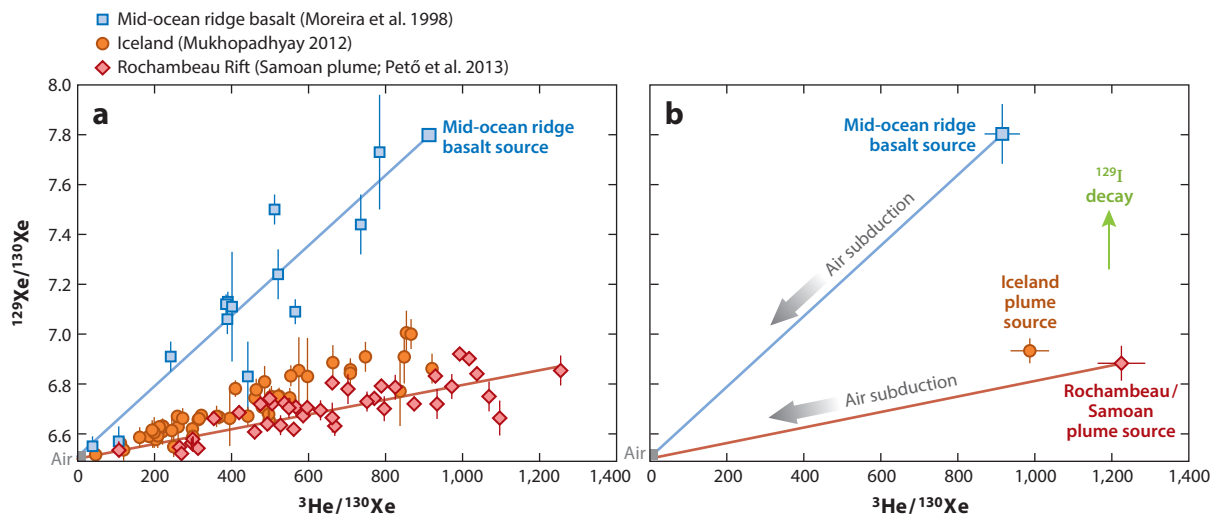


**Figure 7**

Correlation of  $^{129}\text{Xe}$ , produced from the decay of extinct  $^{129}\text{I}$ , with  $^3\text{He}$  for the MORB and plume source compositions. (a) Step-crushing data from the Mid-Atlantic Ridge MORB 21D43 compared to high-precision step-crushing data of basalt glass from the Iceland and Rochambeau Rift (Samoa) plumes. Figure modeled after Pető et al. (2013). (b) Comparison of the MORB source valve with the Iceland and Rochambeau plume sources. Mantle source values are determined by correcting for syn- to post-eruptive atmospheric contamination [e.g., Figure 2 and Pető et al. (2013)]. Two-component mixing in this space is linear, and the observations demonstrate that adding recycled atmospheric Xe to the MORB source cannot generate the plume composition. MORB data are from Moreira et al. (1998), while the Iceland and Lau/Samoa data are from Mukhopadhyay (2012) and Pető et al. (2013), respectively. Abbreviations: He, helium; I, iodine; MORB, mid-ocean ridge basalt; Xe, xenon.

ancient differentiation is still preserved in the modern-day mantle (Mukhopadhyay 2012, Pető et al. 2013). These first-order conclusions were confirmed by Caracausi et al. (2016) from magmatic gas samples derived from the deep mantle in the Eifel volcanic area of Germany.

The observation that differences in isotopic composition produced by extinct radionuclides persist within the mantle to the present day has several important implications for understanding Earth accretion, mantle evolution, and volatile fluxes between Earth reservoirs. The lifetime of  $^{129}\text{I}$  is concurrent with Earth's accretional timescale (e.g., Jacobson et al. 2014). Therefore, differences between plume and MORB  $^{129}\text{Xe}/^{130}\text{Xe}$  were set up during Earth's accretion. The preservation of heterogeneities created during Earth's accretion then requires that Earth's mantle was not chemically homogenized by giant impacts and subsequent magma oceans. Likewise, the preservation of ancient heterogeneities indicates that differences between the plume and MORB source mantles could not have been generated solely through processes associated with plate subduction, mantle convection, or crust mantle differentiation occurring during the past 4.45 Gyr of Earth's history. However, total convective isolation of the plume source from the MORB source is not required. Rather, mixing between the MORB and plume reservoirs was limited, so as to still preserve a difference in Xe isotopic compositions (Mukhopadhyay 2012, Pető et al. 2013).

The ratio of  $^{129}\text{I}$ -derived  $^{129}\text{Xe}$  to  $^{244}\text{Pu}$ -derived fissionogenic  $^{136}\text{Xe}$  ( $^{129}\text{Xe}^*/^{136}\text{Xe}^*_{\text{Pu244}}$ ) provides further confirmation of the antiquity of the reservoir sampled by mantle plumes. From measurements of combined Ne-Ar-Xe isotopes in mantle-derived basalts, the mantle Xe isotopic composition corrected for syn- to post-eruptive atmospheric contamination can be determined (Parai & Mukhopadhyay 2015) (e.g., Figure 2). In the modern mantle, the nine Xe isotopes are a combination of the chondritic Xe acquired by the solid Earth during accretion (Caracausi et al. 2016),

**Extinct radionuclide:** radioactive isotope present during formation of the Solar System but that has since decayed to an effective abundance of zero

radiogenic Xe from  $^{129}\text{I}$ , fissionogenic Xe from  $^{244}\text{Pu}$ , fissionogenic Xe from  $^{238}\text{U}$ , and recycled atmospheric Xe. Each of these five components has a distinct isotopic fingerprint, and there are more isotope ratios than components (**Table 1**). Thus, one may use a linear least squares method to determine the mixing proportions of the five Xe components that best explain the present-day mantle composition (Mukhopadhyay 2012, Parai & Mukhopadhyay 2015, Pető et al. 2013, Tucker et al. 2012). Based on this treatment, the  $^{129}\text{Xe}^*/^{136}\text{Xe}^*_{\text{Pu244}}$  ratio is determined to be  $3^{+0.1}_{-0.2}$  for plumes, lower than the value of  $8.2^{+2.0}_{-1.3}$  for the MORB source (Caracausi et al. 2016, Mukhopadhyay 2012, Parai & Mukhopadhyay 2015, Pető et al. 2013, Tucker et al. 2012).

The  $^{129}\text{Xe}^*/^{136}\text{Xe}^*_{\text{Pu244}}$  ratio can be used to calculate a closure age ( $T$ ) of a reservoir (Pepin & Phinney 1976) based on

$$T = \frac{1}{\lambda_{244} - \lambda_{238}} \times \ln \left[ \frac{(^{129}\text{Xe}^*/^{136}\text{Xe}_{\text{Pu244}}^*)(^{238}\text{U}/^{127}\text{I})_o(^{244}\text{Pu}/^{238}\text{U})_o^{136}\text{Y}_{244}}{(^{129}\text{I}/^{127}\text{I})_o} \right], \quad 1.$$

where  $\lambda_s$  are the decay constants,  $^{136}\text{Y}_{244}$  is the fission yield of  $^{136}\text{Xe}$  from Pu fission,  $^{129}\text{Xe}^*$  is the radiogenic  $^{129}\text{Xe}$  produced from  $^{129}\text{I}$  decay,  $^{136}\text{Xe}_{\text{Pu244}}^*$  is the fissionogenic  $^{136}\text{Xe}$  produced from  $^{244}\text{Pu}$  fission, and the subscript  $o$  refers to the initial value. The formulation yields the age that a reservoir (e.g., the solid Earth or Earth's atmosphere) transitioned from open-system, quantitative Xe loss to closed-system retention of Xe. If the whole mantle had a homogeneous I/Pu ratio, then, based on Equation 1, the higher  $^{129}\text{Xe}^*/^{136}\text{Xe}_{\text{Pu244}}^*$  ratio in the MORB source would imply that the shallower MORB source mantle became closed to significant volatile loss earlier than the deeper plume mantle source (i.e., the deeper mantle continued to lose volatiles after the shallow mantle had stopped losing volatiles) (**Figure 8a**). Such a scenario is physically unrealistic, as mantle outgassing and volatile loss occur at Earth's surface. A simpler and more plausible interpretation of the lower  $^{129}\text{Xe}^*/^{136}\text{Xe}_{\text{Pu244}}^*$  ratio is a lower initial I/Pu ratio for the deeper plume source compared to the shallower MORB source (**Figure 8b**). Since both  $^{129}\text{I}$  and  $^{244}\text{Pu}$  are extinct radionuclides,

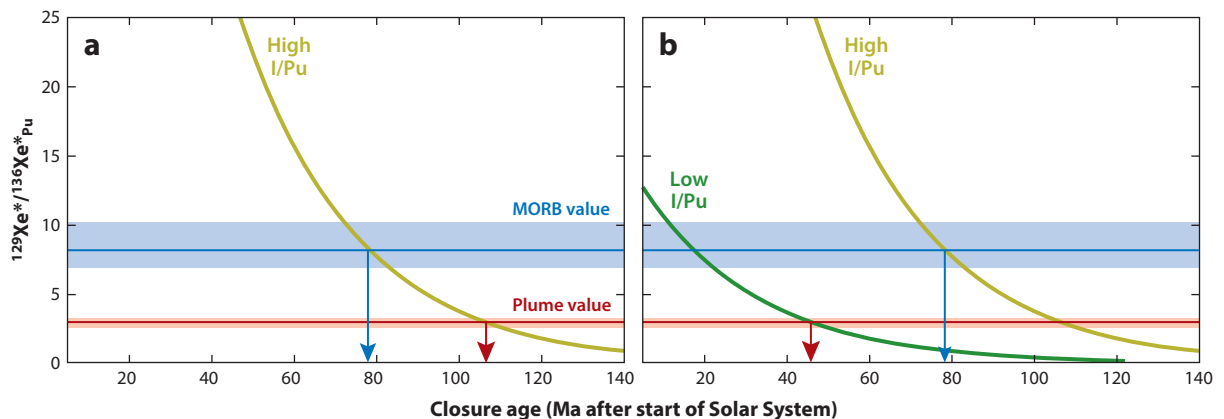


**Figure 8**

Illustrative example showing the mantle closure age for the MORB and plume sources calculated from Equation 1 based on (a) the same I/Pu ratio in both reservoirs and (b) a lower I/Pu ratio in the plume reservoir. Note that stated closure ages calculated here are strongly model dependent, are meant for illustration, and should not be taken to have actual significance. U was taken to be 21 ppb (McDonough & Sun 1995), the Pu/U ratio was taken to be 0.0068 (Hudson et al. 1989), and the high and low I/Pu ratios correspond to bulk silicate Earth contents of 13 ppb and 1 ppb, respectively. The  $^{129}\text{Xe}^*/^{136}\text{Xe}^*_{\text{Pu244}}$  ratio computed for the plume and MORB sources assumes a chondritic starting composition for Xe isotopes in the mantle (Caracausi et al. 2016). The plume average was compiled from data presented by Mukhopadhyay (2012), Pető et al. (2013), and Caracausi et al. (2016). The MORB average is from Parai & Mukhopadhyay (2015). Abbreviations: I, iodine; MORB, mid-ocean ridge basalt; Pu, plutonium; U, uranium; Xe, xenon.

the differences in I/Pu ratios as recorded by MORB and plume source  $^{129}\text{Xe}^*/^{136}\text{Xe}_{\text{Pu}244}^*$  ratios had to be established before the extinction of  $^{244}\text{Pu}$   $\sim 500$  Myr after the start of the Solar System.

Accretional processes have been suggested to drive differences in I/Pu among mantle reservoirs. Since I is a highly volatile element and Pu is a refractory lithophile element, the differences in the  $^{129}\text{Xe}^*/^{136}\text{Xe}_{\text{Pu}244}^*$  ratio between MORB and plume sources have been suggested to reflect heterogeneous volatile accretion, with the initial phase of Earth's accretion being volatile poor compared to the later stages of accretion (Mukhopadhyay 2012, Parai & Mukhopadhyay 2015, Petř et al. 2013). This is consistent with evidence for heterogeneous accretion of other volatile elements including water (e.g., Morbidelli et al. 2012, Rubie et al. 2015, Schonbachler et al. 2010). However, I also becomes siderophile at higher pressures (Armytage et al. 2013, Jackson et al. 2018), and the distinct MORB and plume source I/Pu ratios have been suggested to reflect metal-silicate partitioning of I associated with core formation (Jackson et al. 2018). This interpretation requires earlier giant impacts to develop deep magma oceans with corresponding high-pressure metal-silicate equilibration and later giant impacts, including the Moon-forming impact, to develop shallower magma oceans with lower-pressure metal-silicate equilibration. Whether such a scenario is physically realistic during Earth's accretion remains an open question. Most likely, both heterogeneous volatile accretion and high-pressure core formation contributed to the differences in  $^{129}\text{Xe}^*/^{136}\text{Xe}_{\text{Pu}244}^*$  ratios between plumes and MORBs, although the relative importance of the two processes is currently not entirely clear.

## 7. LONG-TERM MANTLE EVOLUTION AND MANTLE DYNAMICS

Xe isotopes demonstrate that plumes sample a region of the mantle that differentiated from the MORB source mantle  $>4.45$  billion years ago (**Figure 7**). However, this observation should not be used to argue for convective isolation of the plume source from the MORB source. The geochemical observations, including the Xe budget of the mantle, actually prohibit convective isolation of the plume source. In this section, we discuss how differences in noble gas isotope ratios shed light on the long-term evolution of the mantle and mantle structure.

### 7.1. Constraints from Helium Isotopic Compositions

He isotopic ratios ( $^4\text{He}/^3\text{He}$ ) in plumes and MORBs have long formed the backbone for models of mantle structure and evolution. The range of He isotopic ratios in MORBs differs from those measured in plume-derived basalts (e.g., Farley et al. 1992; Graham 2002; Hilton et al. 1999, 2000; Kurz et al. 1982a,b; Moreira 2013; Moreira & Allègre 1998; Mukhopadhyay 2012; Parai et al. 2012; Petř et al. 2013; Poreda & Farley 1992; Trierloff et al. 2000; Tucker et al. 2012). For example, MORBs removed from plume influences typically display a narrow range of  $^4\text{He}/^3\text{He}$  ratios of between  $\sim 80,000$  and  $100,000$  ( $^3\text{He}/^4\text{He}$  ratios of  $\sim 7-9R_A$ , where  $R_A$  is the atmospheric  $^3\text{He}/^4\text{He}$  ratio) (Graham et al. 1992, Kurz et al. 1982b, Moreira & Allègre 1998). In contrast, plume He isotopic signatures vary widely, with  $^4\text{He}/^3\text{He}$  ratios ranging from  $\sim 14,000$  to  $\sim 145,000$  ( $5-50 R_A$ ) (Farley et al. 1992, Graham 2002, Hilton et al. 1999, Kurz & Geist 1999, Kurz et al. 1983, Moreira et al. 1999, Stuart et al. 2003). The low  $^4\text{He}/^3\text{He}$  ratios in plume-derived basalts are associated with  $^{143}\text{Nd}/^{144}\text{Nd}$  ratios that are depleted relative to a chondritic bulk silicate Earth value (Class & Goldstein 2005, Jackson & Carlson 2011, Jackson & Jellinek 2013, Jackson et al. 2010). The combined He-Nd geochemical characteristics in plumes compared to MORBs have been attributed to convective isolation of the plume source for geological periods ( $>1$  Ga) (Class & Goldstein 2005), to a less-processed lower mantle relative to the upper mantle (Gonnermann & Mukhopadhyay 2009), and to sampling a bulk silicate Earth mantle with

nonchondritic samarium (Sm)/Nd ratios (Jackson & Carlson 2011, Jackson & Jellinek 2013, Jackson et al. 2010).

There are several additional models to explain MORB and plume noble gas isotope systematics. For example, low plume  $^4\text{He}/^3\text{He}$  ratios have been attributed to the generation of low  $(\text{U} + \text{Th})/^3\text{He}$  in residues of partial melting (Parman et al. 2005), although more recent determinations of the He partition coefficient (Heber et al. 2007, Jackson et al. 2013) do not support such interpretations. Lee et al. (2010) proposed deep melting over the first 1 Gyr of Earth history to produce dense partial melts, which crystallize and sink to the CMB without degassing, creating a dense, volatile, rich layer at the CMB. Huang et al. (2014) hypothesized that plume He signatures reflect preferential sampling of primitive  $^4\text{He}/^3\text{He}$  frozen into sulfide-rich mafic cumulates generated at  $\sim 3$  Ga or later in association with continent formation. Davies (2010) proposed that reactions between undegassed melts and surrounding mantle peridotite underneath a mid-ocean ridge produce noble gas-rich pyroxenites, which, being more dense than peridotites, sink to the D' layer at the CMB. The suite of explanations put forth to explain the He isotopic ratios runs the gamut from sampling of a reservoir that has experienced minimal processing by partial melting to sampling geologically old ( $> 1$  Ga) signatures generated within the mantle to different mantle-processing rates in the different mantle reservoirs. Thus, additional information, discussed below, is required to interpret the story from He isotopes.

## 7.2. Constraints from Argon and Xenon Isotopic Compositions for a Less-Degassed Plume Source

Ar and Xe isotopic data can be evaluated to help distinguish between the different hypotheses put forth to explain the differences in  $^4\text{He}/^3\text{He}$  ratios between MORBs and plumes. The  $^{40}\text{Ar}/^{36}\text{Ar}$  ratio of the mantle source, which is a function of the time-integrated  $\text{K}/^{36}\text{Ar}$  ratio, is lower in the plume source and higher in the MORB source. Mantle  $^{40}\text{Ar}/^{36}\text{Ar}$  ratios (i.e., measured values corrected for syn- to post-eruptive atmospheric contamination) (**Figure 2**) are 8,000–13,700 for plumes (Colin et al. 2015, Mukhopadhyay 2012, Peron et al. 2016, Petř et al. 2013, Trierloff et al. 2000) and 20,000–50,000 for MORBs (Moreira & Allègre 1998, Parai et al. 2012, Raquin & Moreira 2009, Tucker et al. 2012). The lower time-integrated  $\text{K}/^{36}\text{Ar}$  ratio of the plume source is consistent with sampling of a mantle source that has experienced less processing and less degassing over Earth history than the mantle source of MORBs. However, low  $^{40}\text{Ar}/^{36}\text{Ar}$  ratios in plumes can be equally well explained by preferential incorporation of recycled material with seawater-derived noble gases into the plume source relative to the MORBs (e.g., Holland & Ballentine 2006). This latter scenario is, however, categorically ruled out by Xe data from mantle-derived rocks. If Xe isotopic differences were generated solely by preferential incorporation of recycled atmospheric noble gases into plumes, then MORB and plume Xe isotopic compositions would be colinear with the atmospheric composition in all Xe isotope spaces. The Xe data presented in the previous section demonstrate that plume and MORB sources cannot be related by differential regassing of atmospheric volatiles (**Figures 7 and 8**). Another process must have generated the differences evident in the long-lived radiogenic noble gas isotope systems.

The fissionogenic isotopes of Xe ( $^{131}\text{Xe}$ ,  $^{132}\text{Xe}$ ,  $^{134}\text{Xe}$ , and  $^{136}\text{Xe}$ ) contribute to an emerging portrait of mantle plumes sampling an ancient reservoir that is on average significantly less degassed than the MORB source.  $^{244}\text{Pu}$  and  $^{238}\text{U}$  produce the four fissionogenic Xe isotopes in different proportions, and fissionogenic Xe yields from Pu are significantly larger than from U. Consequently, a reservoir that remains completely closed to volatile loss over Earth's history has a  $^{136}\text{Xe}_{\text{Pu}}/(^{136}\text{Xe}_{\text{Pu}} + ^{136}\text{Xe}_{\text{U}})$  ratio of approximately 0.97 (Azbel & Tolstikhin 1993, Tolstikhin & O'Nions 1996, Tolstikhin et al. 2006). Reservoirs that underwent extensive degassing over

the past 4 Gyr, after  $^{244}\text{Pu}$  became extinct, have lost a significant fraction of the Pu-produced fissiogenic Xe and have fissiogenic Xe resupplied by spontaneous fission of  $^{238}\text{U}$ . As a result,  $^{136}\text{Xe}_{\text{Pu}}/(^{136}\text{Xe}_{\text{Pu}}+^{136}\text{Xe}_{\text{U}})$  in degassed reservoirs is much less than 0.97.

The MORB source uniformly exhibits a low  $^{136}\text{Xe}_{\text{Pu}}/(^{136}\text{Xe}_{\text{Pu}}+^{136}\text{Xe}_{\text{U}})$  ratio relative to the plume source (Caracausi et al. 2016, Mukhopadhyay 2012, Parai & Mukhopadhyay 2015, Petó et al. 2013, Tucker et al. 2012.) (**Figures 5 and 8**). The MORB source has an error-weighted average  $^{136}\text{Xe}_{\text{Pu}}/(^{136}\text{Xe}_{\text{Pu}}+^{136}\text{Xe}_{\text{U}})$  ratio of  $0.28^{+0.11}_{-0.10}$  using chondritic Xe as the primordial Xe component in the MORB source (Parai & Mukhopadhyay 2015). On the other hand, plume sources have an error-weighted average  $^{136}\text{Xe}_{\text{Pu}}/(^{136}\text{Xe}_{\text{Pu}}+^{136}\text{Xe}_{\text{U}})$  ratio of  $0.96^{+0.03}_{-0.18}$  using chondritic Xe as the primordial Xe component. The very large difference in  $^{136}\text{Xe}_{\text{Pu}}/(^{136}\text{Xe}_{\text{Pu}}+^{136}\text{Xe}_{\text{U}})$  ratios leaves little doubt that the MORB source has uniformly experienced a much greater extent of integrated degassing associated with long-term mantle processing relative to the plume source. We note that this observation is based on only the Xe isotopic compositions, and it is independent of absolute concentrations of any element.

### 7.3. Constraints from Argon and Xenon for Recycling of Atmospheric Noble Gases

The lower degree of degassing of the plume source is, however, not the only message when it comes to interpreting the noble gas observations. The Ar and Xe compositions of both the MORB and the plume sources point to significant injection of recycled atmospheric heavy noble gases. Subduction zones were long thought to be efficient barriers to the recycling of noble gases into the deep mantle (e.g., Staudacher & Allègre 1988). One of the most fundamental recent developments in the field came from Holland & Ballentine (2006), who used the full suite of noble gas (He, Ne, Ar, Kr, and Xe) measurements in  $\text{CO}_2$  gases from the Bravo Dome gas field in New Mexico, USA, to demonstrate that the relative abundance pattern of the noble gases in both MORBs and the well-gas samples was similar to that of seawater. This observation suggested substantial subduction of seawater-derived noble gases into the convective mantle such that  $\sim 80\%$  of the primordial Xe isotopes ( $^{124}\text{Xe}$ ,  $^{126}\text{Xe}$ ,  $^{128}\text{Xe}$ , and  $^{130}\text{Xe}$ ) were recycled and  $\sim 100\%$  of the primordial Ar isotopes ( $^{36}\text{Ar}$ ,  $^{38}\text{Ar}$ ) were of recycled origin. Subsequent work has confirmed the recycling of atmospheric Ar and Xe into the mantle (Kendrick et al. 2011, 2013; Sumino et al. 2010), and recent studies have also used Xe isotope systematics to demonstrate that 80–90% of the Xe in both plumes and MORBs is recycled atmosphere-derived Xe (Parai & Mukhopadhyay 2015, Tucker et al. 2012). We emphasize, however, that differential degassing cannot explain differences between MORB and plume noble gas compositions.

The observation of ancient Xe signatures, combined with a primarily recycled Xe budget, requires that plumes cannot sample only an unprocessed, ancient (pre-4.45 Ga) region of the mantle. Significant recycled material must be mixed in with the ancient mantle source, such that the plume source is not convectively isolated. Therefore, plumes with primitive He isotopic compositions (low  $^4\text{He}/^3\text{He}$ ) do not reflect sampling a mantle with bulk silicate Earth composition. Hence, major and trace element compositions, along with lithophile isotopic ratios, of samples with primitive He isotopic compositions (Jackson & Carlson 2011, Jackson & Jellinek 2013) should not be taken to represent the composition of bulk silicate Earth. Gonnermann & Mukhopadhyay (2009) demonstrated that mantle He-Nd systematics can be explained by differential incorporation of He-poor recycled slabs with high Sm/Nd ratios into both the MORB and plume sources over Earth history. In this case, degassed, trace element-depleted slabs are incorporated into the plume source over time. The slabs depleted in primordial  $^3\text{He}$  mix with the ancient reservoir, which dilutes the concentrations of noble gases and decreases the efficiency of subsequent mantle

degassing while imparting depleted lithophile compositions to the mantle reservoir. Quantitative modeling suggests that mantle noble gas signatures can be attributed to a mantle reservoir that has continuously evolved and progressively been depleted through incorporation of recycled slabs (Gonnermann & Mukhopadhyay 2009). Accordingly, low  $^4\text{He}/^3\text{He}$  ratios may be preserved in a mantle reservoir that is not reflective of the bulk silicate Earth. The mixing of slabs and ancient reservoirs should generate a continuum of compositions between relatively well-mixed assemblages and incompletely mixed recycled slabs. The He isotopic difference between plume and MORB sources would then be related to the greater degree of processing and mixing for MORBs; direct mixing between plume and MORB sources has to be limited to generate the isotopic differences in He and Nd (Gonnermann & Mukhopadhyay 2009), although limited direct mixing is also a requirement for preserving differences in radiogenic Xe produced by extinct radionuclides.

Finally, we note that the recycling of atmospheric Ar and Xe back into the mantle was an important paradigm shift since it introduced a different way to interpret variations in observed Xe isotopic ratios. For example, variations in  $^{40}\text{Ar}/^{36}\text{Ar}$  and  $^{129}\text{Xe}/^{130}\text{Xe}$  ratios in mantle-derived samples do not all necessarily need to arise from preservation of mantle domains with different melt and gas extraction histories. Instead,  $^{40}\text{Ar}/^{36}\text{Ar}$  and  $^{129}\text{Xe}/^{130}\text{Xe}$  variations could arise from variable amounts of recycled atmospheric Ar and Xe in the mantle. While the broad differences between MORB and plume Xe isotope systematics cannot be attributed to differential injection of atmospheric gases (Figures 7 and 8), inefficient mixing within either mantle reservoir means that variability among various plumes and among MORB sources may be observed. Parai et al. (2012) found that after explicitly correcting for syn- to posteruptive atmospheric contamination, there were dramatic variations in  $^{40}\text{Ar}/^{36}\text{Ar}$  and  $^{129}\text{Xe}/^{130}\text{Xe}$  ratios in MORBs not influenced by plumes (Figure 9). The large variations, which span 70% and 80% of the entire mantle range for  $^{40}\text{Ar}/^{36}\text{Ar}$  and  $^{129}\text{Xe}/^{130}\text{Xe}$  ratios, respectively, could be explained by heterogeneous incorporation of recycled atmospheric noble gases into the MORB source (Parai et al. 2012). These large variations in Ar and Xe isotopic ratios are associated with very limited  $^4\text{He}/^3\text{He}$  variability that is well within the normal range from MORBs and is not consistent with differential long-term processing history. Hence, the broad homogeneity noted in MORB He isotopic compositions (Graham 2002; Graham et al. 1992; Kurz et al. 1982a,b) does not indicate a homogeneous MORB source; the persistence of large Ar and Xe isotopic variations generated by heterogeneous

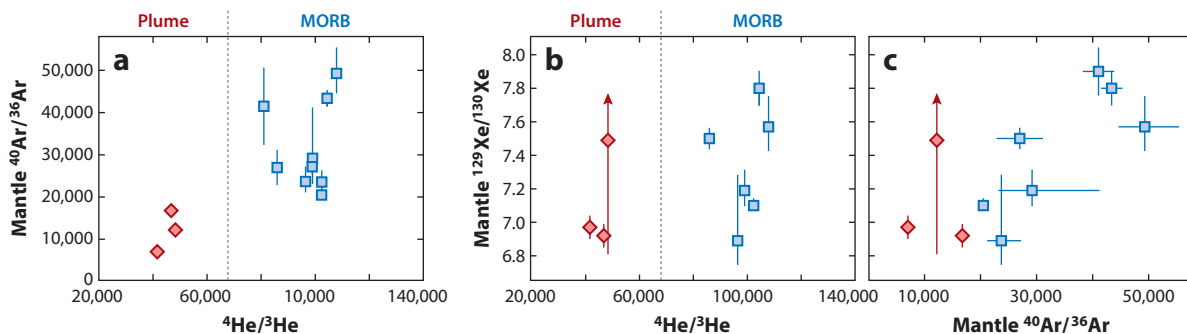


**Figure 9**

Covariations in (a) Ar and (b) Xe isotopes against He isotopes and (c) covariation of Ar with Xe isotopes. Mantle  $^{40}\text{Ar}/^{36}\text{Ar}$  and mantle  $^{129}\text{Xe}/^{130}\text{Xe}$  ratios reflect measured ratios corrected for syn- to posteruptive atmospheric contamination (e.g., Figure 2). Note that there are large variations in Ar and Xe isotopes with limited He isotopic variability in MORBs, while there seems to be a better covariation of Ar and Xe isotopes (c) consistent with regassing driving variation in Ar and Xe isotopes. Figure updated from Parai et al. (2012). Abbreviations: Ar, argon; He, helium; MORB, mid-ocean ridge basalt; Xe, xenon.

regassing reflects the signature of inefficient homogenization of recycled material in the MORB source. The inherent variations in the Ar and Xe isotopic ratios in MORB and plume sources reflect the ongoing incorporation of recycled material into distinct ancient mantle reservoirs (Parai & Mukhopadhyay 2015).

#### 7.4. An Emerging Picture of Mantle Structure

Consideration of the full suite of noble gases paints a complex picture of the origin and evolution of the MORB and plume source regions. While differences between the MORB source mantle and plume source mantle require ancient (pre-4.45 Ga) differentiation and degassing events (Figure 7), significant atmospheric Ar and Xe have been injected and incorporated into both these mantle sources. The observation requires incorporation of recycled materials into mantle plumes, which precludes the use of plume compositions from Iceland and Samoa as records of a bulk silicate Earth composition. The association of primitive He (low  $^4\text{He}/^3\text{He}$ ) ratios with depleted Nd and strontium (Sr) isotopic compositions is therefore best ascribed to the same process of incorporating recycled material into the plume source (e.g., Gonnermann & Mukhopadhyay 2009). The differences between MORB and plume source He, Sr, and Nd isotopic signatures may relate to greater processing of the shallower MORB source. Seismic evidence indicates that the vast majority of slabs stagnate at depths of 600–1,000 km (Fukao & Obayashi 2013), upwelling plumes appear to partially stagnate and deflect at 1,000 km (French & Romanowicz 2015), and the spatial patterns of shear wave velocity anomalies are different on either side of the transition zone (Kustowski et al. 2008). These observations suggest a convection regime that may be somewhere between the end-member scenarios of whole mantle and layered mantle convection (Figure 10).

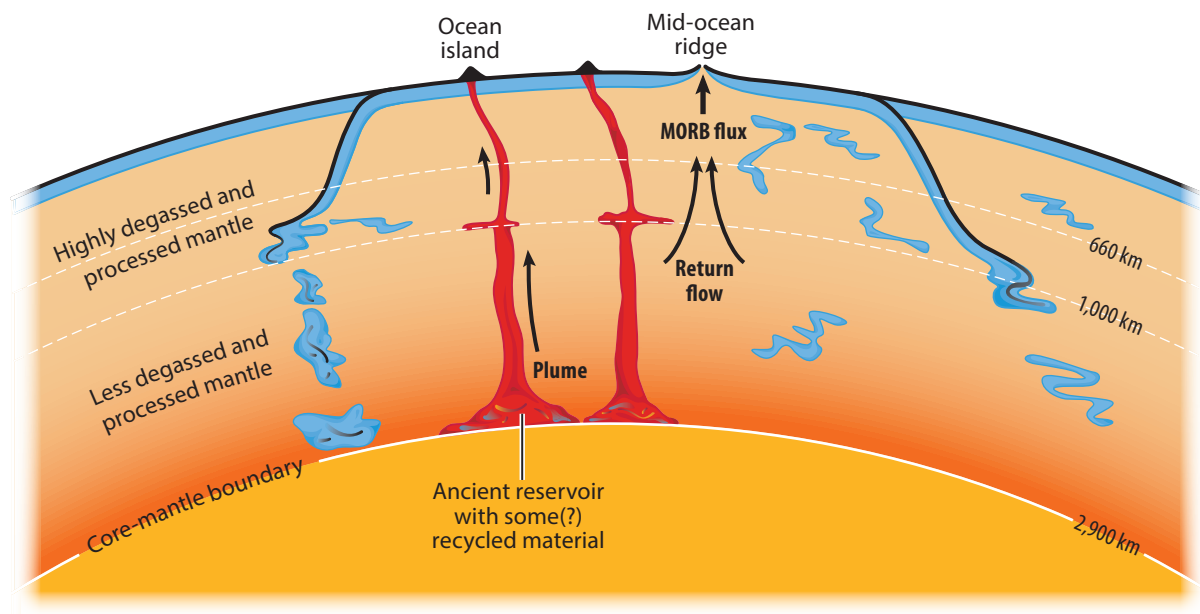


**Figure 10**

An emerging view of mantle structure that may be compatible with most geochemical and geophysical observations. Abbreviation: MORB, mid-ocean ridge basalt.

## 8. SUMMARY

In the past decade, several important advances in earth science have been made through studies involving noble gases. These include evidence for the preservation of deep mantle heterogeneities dating back to Earth's accretion, evidence of heterogeneous volatile accretion with early accretion being volatile poor, the observation that primordial noble gases in the atmosphere cannot be derived from mantle outgassing, the observation of mass fractionating Xe loss from the atmosphere during the Hadean and Archean, the discovery of the progenitor of atmospheric Xe in comets, evidence for the transport of atmospheric noble gases associated with hydrous phases back into the mantle, and the realization that differences in MORB and plume geochemistry can be explained through the lens of a less-degassed versus more-degassed reservoir—the bulk composition of plumes does not reflect a bulk silicate Earth composition. Looking ahead, key areas for improvement include measurement precision, techniques to reduce shallow-level air contamination in terrestrial samples, determination of the high P-T behavior of noble gases, and better integration of the full spectrum of noble gas isotopes into realistic geodynamic models.

## DISCLOSURE STATEMENT

The authors are not aware of any affiliations, memberships, funding, or financial holdings that might be perceived as affecting the objectivity of this review.

## ACKNOWLEDGMENTS

We thank an anonymous reviewer for comments that helped improve this article. There is a long and rich history of scholarship in noble gas geochemistry. We apologize for any unintended omissions, as we were able to cite only the most relevant publications. This work was supported by National Science Foundation grant number OCE 0929193.

## LITERATURE CITED

- Albarède F. 2009. Volatile accretion history of the terrestrial planets and dynamic implications. *Nature* 461:1227–33
- Alexander CMO'D. 2017. The origin of inner Solar System water. *Philos. Trans. R. Soc. A* 375:20150384
- Alexander CMO'D, Bowden R, Fodgel ML, Howard KT, Herd CDK, Nittler LR. 2012. The provenances of asteroids, and their contributions to the volatile inventories of the terrestrial planets. *Science* 337:721–23
- Alexander CMO'D, Cody GD, De Gregorio BT, Nittler LR, Stroud RM. 2017. The nature, origin and modification of insoluble organic matter in chondrites, the major source of Earth's C and N. *Chem. Erde Geochem.* 77:227–56
- Allègre CJ, Staudacher T, Sarda P. 1987. Rare gas systematics: formation of the atmosphere, evolution and structure of the Earth's mantle. *Earth Planet. Sci. Lett.* 81:127–50
- Allègre CJ, Staudacher T, Sarda P, Kurz M. 1983. Constraints on evolution of Earth's mantle from rare gas systematics. *Nature* 303:762–66
- Altwegg K, Balsiger H, Bar-Nun A, Berthelier JJ, Bieler A, et al. 2015. 67P/Churyumov-Gerasimenko, a Jupiter family comet with a high D/H ratio. *Science* 347:1261952
- Armytage RM, Jephcoat AP, Bouhifd MA, Porcelli D. 2013. Metal–silicate partitioning of iodine at high pressures and temperatures: implications for the Earth's core and  $^{129}\text{Xe}$  budgets. *Earth Planet. Sci. Lett.* 373:140–49
- Avice G, Marty B. 2014. The iodine–plutonium–xenon age of the Moon–Earth system revisited. *Philos. Trans. R. Soc. A* 372:20130260
- Avice G, Marty B, Burgess R. 2017. The origin and degassing history of the Earth's atmosphere revealed by Archean xenon. *Nat. Commun.* 8:15455

- Azbel IY, Tolstikhin I. 1993. Accretion and early degassing of the Earth: constraints from Pu-U-I-Xe isotopic systematics. *Meteoritics* 28:609–21
- Ballentine CJ, Marty B, Sherwood LB, Cassidy M. 2005. Neon isotopes constrain convection and volatile origin in the Earth's mantle. *Nature* 433:33–38
- Bar-Nun A, Notesco G, Owen T. 2007. Trapping of N<sub>2</sub>, CO and Ar in amorphous ice—application to comets. *Icarus* 190:655–59
- Becker TW, Kellogg JB, O'Connell RJ. 1999. Thermal constraints on the survival of primitive blobs in the lower mantle. *Earth Planet. Sci. Lett.* 171:351–65
- Bockelée-Morvan D, Gautier D, Lis DC, Young K, Keene J, et al. 1998. Deuterated water in comet C 1996 B2 (Hyakutake) and its implications for the origin of comets. *Icarus* 133:147–62
- Bouhifd MA, Jephcoat AP, Heber VS, Kelley SP. 2013. Helium in Earth's early core. *Nat. Geosci.* 6:982–86
- Brooker RA, Du Z, Blundy JD, Kelley SP, Allan NL, et al. 2003. The 'zero charge' partitioning behaviour of noble gases during mantle melting. *Nature* 423:738–41
- Burnard P, Harrison D, Turner G, Nesbitt RW. 2003. Degassing and contamination of noble gases in Mid-Atlantic Ridge basalts. *Geochem. Geophys. Geosyst.* 4:1002
- Caffee MW, Hudson GB, Velsko C, Huss GR, Alexander EC Jr., Chivas AR. 1999. Primordial noble gases from Earth's mantle: identification of a primitive volatile component. *Science* 285:2115–18
- Caracausi A, Avice G, Burnard PG, Furi E, Marty B. 2016. Chondritic xenon in the Earth's mantle. *Nature* 533:82–85
- Class C, Goldstein SL. 2005. Evolution of helium isotopes in the Earth's mantle. *Nature* 425:1107–12
- Colin A, Burnard P, Marty B. 2013. Mechanisms of magma degassing at mid-oceanic ridges and the local volatile composition (<sup>4</sup>He–<sup>40</sup>Ar\*–CO<sub>2</sub>) of the mantle by laser ablation analysis of individual MORB vesicles. *Earth Planet. Sci. Lett.* 261:183–94
- Colin A, Moreira M, Gautheron C, Burnard P. 2015. Constraints on the noble gas composition of the deep mantle by bubble-by-bubble analysis of a volcanic glass sample from Iceland. *Chem. Geol.* 417:173–83
- Coltice N, Moreira M, Hernlund J, Labrosse S. 2011. Crystallization of a basal magma ocean recorded by helium and neon. *Earth Planet. Sci. Lett.* 308:193–99
- Dauphas N. 2003. The dual origin of the terrestrial atmosphere. *Icarus* 165:326–39
- Dauphas N, Morbidelli A. 2014. The atmosphere—history. In *Treatise on Geochemistry*, Vol. 6, ed. DE Canfield, J Farquhar, JF Kasting, pp. 1–35. Amsterdam: Elsevier. 2nd ed.
- Dauphas N, Pourmand A. 2011. Hf–W–Th evidence for rapid growth of Mars and its status as a planetary embryo. *Nature* 473:489–92
- Davies GF. 2010. Noble gases in the dynamic mantle. *Geochem. Geophys. Geosyst.* 11:Q03005
- Elkins-Tanton LT. 2008. Linked magma ocean solidification and atmospheric growth for Earth and Mars. *Earth Planet. Sci. Lett.* 271:181–91
- Erkaev NV, Lammer H, Elkins-Tanton LT, Stokl A, Odert P, et al. 2014. Escape of the martian protoatmosphere and initial water inventory. *Planet. Space Sci.* 98:106–19
- Farley KA, Natland JH, Craig H. 1992. Binary mixing of enriched and undegassed (primitive?) mantle components (He, Sr, Nd, Pb) in Samoan lavas. *Earth Planet. Sci. Lett.* 111:183–99
- Fisher DE. 1983. Rare gases from the undepleted mantle? *Nature* 305:298–300
- French SW, Romanowicz B. 2015. Broad plumes rooted at the base of the Earth's mantle beneath major hotspots. *Nature* 525:95–99
- Fukao Y, Obayashi M. 2013. Subducted slabs stagnant above, penetrating through, and trapped below the 660 km discontinuity. *J. Geophys. Res. Solid Earth* 118:5920–38
- Genda H, Abe Y. 2005. Enhanced atmospheric loss on protoplanets at the giant impact phase in the presence of oceans. *Nature* 433:842–44
- Gonnermann HM, Mukhopadhyay S. 2009. Preserving noble gases in a convecting mantle. *Nature* 459:560–63
- Graham DW. 2002. Noble gas isotope geochemistry of mid-ocean ridge and ocean island basalts: characterization of mantle source reservoirs. *Rev. Mineral. Geochem.* 47:247–318
- Graham DW, Jenkins WJ, Schilling JG, Thompson G, Kurz MD, Humphris SE. 1992. Helium isotope geochemistry of midocean ridge basalts from the South Atlantic. *Earth Planet. Sci. Lett.* 110:133–47
- Halliday AN. 2013. The origins of volatiles in the terrestrial planets. *Geochim. Cosmochim. Acta* 105:146–71

- Hanyu T, Dunai TJ, Davies GR, Kaneoka I, Nohda S, Uto K. 2001. Noble gas study of the Reunion hotspot: evidence for distinct less-degassed mantle sources. *Earth Planet. Sci. Lett.* 193:83–98
- Harper CL, Jacobsen SB. 1996. Noble gases and Earth's accretion. *Science* 273:1814–18
- Harrison D, Burnard P, Turner G. 1999. Noble gas behaviour and composition in the mantle: constraints from the Iceland Plume. *Earth Planet. Sci. Lett.* 171:199–207
- Heber VS, Baur H, Bochsler P, McKeegan KD, Neugebauer M, et al. 2012. Isotopic mass fractionation of solar wind: evidence from fast and slow solar wind collected by the *Genesis* mission. *Astrophys. J.* 759:121
- Heber VS, Brooker RA, Kelley SP, Wood BJ. 2007. Crystal-melt partitioning of noble gases (helium, neon, argon, krypton, and xenon) for olivine and clinopyroxene. *Geochim. Cosmochim. Acta* 71:1041–61
- Hennecke EW, Manuel OK. 1975. Noble gases in an Hawaiian xenolith. *Nature* 257:778–80
- Hilton DR, Grönvold K, Macpherson CG, Castillo PR. 1999. Extreme  $^3\text{He}/^4\text{He}$  ratios in northwest Iceland: constraining the common component in mantle plumes. *Earth Planet. Sci. Lett.* 173:53–60
- Hilton DR, Macpherson CG, Elliott TR. 2000. Helium isotope ratios in mafic phenocrysts and geothermal fluids from La Palma, the Canary Islands (Spain): implications for HIMU mantle sources. *Geochim. Cosmochim. Acta* 64:2119–32
- Hirschmann MM. 2016. Constraints on the early delivery and fractionation of Earth's major volatiles from C/H, C/N and C/S ratios. *Am. Mineral.* 101:540–53
- Hiyagon H, Ozima M, Marty B, Zashu S, Sakai H. 1992. Noble gases in submarine glasses from mid-oceanic ridges and Loihi seamount: constraints on the early history of the Earth. *Geochim. Cosmochim. Acta* 56:1301–16
- Holland G, Ballentine CJ. 2006. Seawater subduction controls the heavy noble gas composition of the mantle. *Nature* 441:186–91
- Holland G, Cassidy M, Ballentine CJ. 2009. Meteorite Kr in Earth's mantle suggests a late accretionary source for the atmosphere. *Science* 326:1522–25
- Honda M, McDougall I. 1998. Primordial helium and neon in the Earth—a speculation on early degassing. *Geophys. Res. Lett.* 25:1951–54
- Honda M, McDougall I, Patterson DB, Doulgeris A, Clague DA. 1991. Possible solar noble-gas component in Hawaiian basalts. *Nature* 349:149–51
- Honda M, McDougall I, Patterson DB, Doulgeris A, Clague DA. 1993. Noble gases in submarine pillow basalt glasses from Loihi and Kilauea, Hawaii—a solar component in the Earth. *Geochim. Cosmochim. Acta* 57:859–74
- Huang S, Lee C-TA, Yin Q-Z. 2014. Missing lead and high  $^3\text{He}/^4\text{He}$  in ancient sulfides associated with continental crust formation. *Sci. Rep.* 4:5314
- Hudson GB, Kennedy BM, Podosek FA, Hohenberg CM. 1989. The early solar system abundance of  $^{244}\text{Pu}$  as inferred from the St. Severin chondrite. In *Proceedings of the 19th Lunar Planetary Science Conference*, pp. 547–57. Cambridge, UK: Cambridge Univ. Press
- Jackson CRM, Bennett NR, Du Z, Cottrell E, Fei Y. 2018. Early episodes of high-pressure core formation preserved in plume mantle. *Nature* 593:491–95
- Jackson CRM, Parman SW, Kelley SP, Cooper RF. 2013. Constraints on light noble gas partitioning at the conditions of spinel-peridotite melting. *Earth Planet. Sci. Lett.* 384:178–87
- Jackson MG, Carlson RW. 2011. An ancient recipe for flood-basalt genesis. *Nature* 476:316–19
- Jackson MG, Carlson RW, Kurz MD, Kempton PD, Francis D, Blusztajn J. 2010. Evidence for the survival of the oldest terrestrial mantle reservoir. *Nature* 466:853–56
- Jackson MG, Jellinek AM. 2013. Major and trace element composition of the high  $^3\text{He}/^4\text{He}$  mantle: implications for the composition of a nonchondritic Earth. *Geochim. Geophys. Geosyst.* 14:2954–76
- Jacobson SA, Morbidelli A. 2014. Lunar and terrestrial planet formation in the Grand Tack scenario. *Philos. Trans. R. Soc. A* 372:20130174
- Jacobson SA, Morbidelli A, Raymond SN, O'Brien DP, Walsh KJ. 2014. Highly siderophile elements in Earth's mantle as a clock for the Moon-forming impact. *Nature* 508:84–87
- Jehin E, Manfroid J, Hutsemekers D, Arpigny C, Zucconi JM. 2009. Isotopic ratios in comets: status and perspectives. *Earth Moon Planets* 105:167–80
- Jephcoat AP. 1998. Rare-gas solids in the Earth's deep interior. *Nature* 393:355–58

- Kaneoka I, Takaoka N. 1978. Excess  $^{129}\text{Xe}$  and high  $^3\text{He}/^4\text{He}$  ratios in olivine phenocrysts of Kapuho lava and xenolithic dunites from Hawaii. *Earth Planet. Sci. Lett.* 39:382–86
- Káráson H, Van Der Hilst RD. 2000. Constraints on mantle convection from seismic tomography. *Geophys. Monogr.* 121:277–88
- Kendrick MA, Honda M, Pettke T, Scambelluri M, Phillips D, Giuliani A. 2013. Subduction zone fluxes of halogens and noble gases in seafloor and forearc serpentinites. *Earth Planet. Sci. Lett.* 365:86–96
- Kendrick MA, Scambelluri M, Honda M, Phillips D. 2011. High abundances of noble gas and chlorine delivered to the mantle by serpentinite subduction. *Nat. Geosci.* 4:807–12
- Kunz J, Staudacher T, Allègre CJ. 1998. Plutonium-fission xenon found in Earth's mantle. *Science* 280:877–80
- Kurz MD, Curtice J, Fornari D, Geist D, Moreira M. 2009. Primitive neon from the center of the Galápagos hotspot. *Earth Planet. Sci. Lett.* 286:23–34
- Kurz MD, Geist D. 1999. Dynamics of the Galapagos hotspot from helium isotope geochemistry. *Geochim. Cosmochim. Acta* 63:4139–56
- Kurz MD, Jenkins WJ, Hart SR. 1982a. Helium isotopic systematics of oceanic islands and mantle heterogeneity. *Nature* 297:43–47
- Kurz MD, Jenkins WJ, Hart SR, Clague D. 1983. Helium isotopic variations in volcanic rocks from Loihi Seamount and the island of Hawaii. *Earth Planet. Sci. Lett.* 66:388–406
- Kurz MD, Jenkins WJ, Schilling JG, Hart SR. 1982b. Helium isotopic variations in the mantle beneath the central North Atlantic Ocean. *Earth Planet. Sci. Lett.* 58:1–14
- Kustowski B, Ekström G, Dziewoński AM. 2008. Anisotropic shear-wave velocity structure of the Earth's mantle: a global model. *J. Geophys. Res.* 113(B6):B06306
- Labrosse S, Hernlund JW, Coltice N. 2007. A crystallizing dense magma ocean at the base of the Earth's mantle. *Nature* 450:866–69
- Lee C-TA, Luffi P, Hoink T, Li J, Dasgupta R, Hernlund J. 2010. Upside-down differentiation and generation of a 'primordial' lower mantle. *Nature* 463:930–33
- Lewis RS, Srinivasan B, Anders E. 1975. Host phase of a strange xenon component in Allende. *Science* 190:1251–62
- Lodders K, Fegley B Jr. 1998. *The Planetary Scientist's Companion*. New York: Oxford Univ. Press
- Manfroid J, Jehin E, Hutsemékers D, Cochran A, Zucconi JM, et al. 2009. The CN isotopic ratios in comets. *Astron. Astrophys.* 503:961–66
- Marty B. 1989. Neon and xenon isotopes in MORB: implications for the earth-atmosphere evolution. *Earth Planet. Sci. Lett.* 94:45–56
- Marty B. 2012. The origins and concentrations of water, carbon, nitrogen and noble gases on Earth. *Earth Planet. Sci. Lett.* 313:56–66
- Marty B, Altwegg K, Balsiger H, Bar-Nun A, Bekaert DV, et al. 2017. Xenon isotopes in 67P/Churyumov-Gerasimenko show that comets contributed to Earth's atmosphere. *Science* 356:1069–72
- Marty B, Avicé G, Yuji S, Altwegg K, Balsiger H, et al. 2016. Origin of volatile elements (H, C, N, noble gases) on Earth and Mars in light of recent results from the ROSETTA cometary mission. *Earth Planet. Sci. Lett.* 441:91–102
- Mazor E, Heymann D, Anders E. 1970. Noble gases in carbonaceous chondrites. *Geochim. Cosmochim. Acta* 34:781–824
- McDonough WF, Sun SS. 1995. The composition of the Earth. *Chem. Geol.* 120:223–53
- Meech KJ, Pittichova J, Bar-Nun A, Natesco G, Laufer D, et al. 2009. Activity of comets at large heliocentric distances pre-perihelion. *Icarus* 201:719–39
- Meier R, Owen TC, Jewitt DC, Matthews HE, Senay M, et al. 1998. Deuterium in comet C/1995 O1 (Hale-Bopp): detection of DCN. *Science* 279:1707–10
- Mizuno H, Nakazawa K, Hayashi C. 1980. Dissolution of the primordial rare gases into the molten Earth's material. *Earth Planet. Sci. Lett.* 50:202–10
- Morbidelli A, Lunine JL, O'Brien DP, Raymond SN, Walsh KJ. 2012. Building terrestrial planets. *Annu. Rev. Earth Planet. Sci.* 40:251–75
- Morbidelli A, Wood B. 2015. Late accretion and the late veneer. In *The Early Earth: Accretion and Differentiation*, ed. J Badro, M Walters, pp. 159–83. Washington, DC: Am. Geophys. Union

- Moreira M. 2013. Noble gas constraints on the origin and evolution of Earth's volatiles. *Geochem. Perspect.* 2:229–403
- Moreira M, Allègre CJ. 1998. Helium–neon systematics and the structure of the mantle. *Chem. Geol.* 147:53–59
- Moreira M, Charnoz S. 2016. The origin of the neon isotopes in chondrites and on Earth. *Earth Planet. Sci. Lett.* 433:249–56
- Moreira M, Doucelance R, Kurz MD, Dupre B, Allègre CJ. 1999. Helium and lead isotope geochemistry of the Azores Archipelago. *Earth Planet. Sci. Lett.* 169:189–205
- Moreira M, Kunz J, Allègre C. 1998. Rare gas systematics in popping rock: isotopic and elemental compositions in the upper mantle. *Science* 279:1178–81
- Mosenfelder JL, Asimow PD, Frost DJ, Rubie DC, Ahrens TJ. 2009. The MgSiO<sub>3</sub> system at high pressure: thermodynamic properties of perovskite, postperovskite, and melt from global inversion of shock and static compression data. *J. Geophys. Res.* 114(B1):B01203
- Mukhopadhyay S. 2012. Early differentiation and volatile accretion recorded in deep mantle neon and xenon. *Nature* 486:101–4
- Mukhopadhyay S, Parai R, Tucker J, Middelton JL, Langmuir CH. 2015. *Early and long-term mantle processing rates derived from xenon isotopes*. Paper presented at the American Geophysical Union Fall Meeting, San Francisco, CA, Dec. 14–15
- Nakajima M, Stevenson DJ. 2015. Melting and mixing states of the Earth's mantle after the Moon-forming impact. *Earth Planet. Sci. Lett.* 427:286–95
- Notesco G, Bar-Nun A, Owen T. 2003. Gas trapping in water ice at very low deposition rates and implications for comets. *Icarus* 162:183–89
- O'Brien DP, Morbidelli A, Levison HF. 2006. Terrestrial planet formation with strong dynamical friction. *Icarus* 184:39–58
- Ott U. 2014. Planetary and pre-solar noble gases in meteorites. *Chem. Erde* 74:519–44
- Ozima M, Podosek FA. 2002. *Noble Gas Geochemistry*. Cambridge, UK: Cambridge Univ. Press. 2nd ed.
- Pahlevan K, Stevenson DJ. 2007. Equilibration in the aftermath of the lunar-forming giant impact. *Earth Planet. Sci. Lett.* 262:438–49
- Parai R, Mukhopadhyay S. 2015. The evolution of MORB and plume mantle volatile budgets: constraints from fission Xe isotopes in Southwest Indian Ridge basalts. *Geochem. Geophys. Geosyst.* 16:719–35
- Parai R, Mukhopadhyay S, Standish JJ. 2012. Heterogeneous upper mantle Ne, Ar and Xe isotopic compositions and a possible Dupal noble gas signature recorded in basalts from the Southwest Indian Ridge. *Earth Planet. Sci. Lett.* 359:227–39
- Parman SW, Kurz MD, Hart SR, Grove TL. 2005. Helium solubility in olivine and implications for high <sup>3</sup>He/<sup>4</sup>He in ocean island basalts. *Nature* 437:1140–43
- Pepin RO. 1991. On the origin and early evolution of terrestrial planet atmospheres and meteoritic volatiles. *Icarus* 92:2–79
- Pepin RO, Phinney D. 1976. The formation interval of the Earth. *Abstr. Lunar Planet. Sci. Conf.* 7:682–84
- Pepin RO, Porcelli D. 2002. Origin of noble gases in the terrestrial planets. *Rev. Mineral. Geochem.* 47:191–246
- Pepin RO, Porcelli D. 2006. Xenon isotope systematics, giant impacts, and mantle degassing on the early Earth. *Earth Planet. Sci. Lett.* 250:470–85
- Peron S, Moreira M, Agranier A. 2018. Origin of light noble gases (He, Ne, and Ar) on Earth: a review. *Geochem. Geophys. Geosyst.* 19:979–96
- Peron S, Moreira M, Colin A, Arbaret L, Putlitz B, Kurz MD. 2016. Neon isotopic composition of the mantle constrained by single vesicle analyses. *Earth Planet. Sci. Lett.* 449:145–54
- Peron S, Moreira M, Putlitz B, Kurz MD. 2017. Solar wind implantation supplied light volatiles during the first stage of Earth accretion. *Geochem. Perspect. Lett.* 3:151–59
- Petó M, Mukhopadhyay S, Kelley KA. 2013. Heterogeneities from the first 100 million years recorded in deep mantle noble gases from the Northern Lau Back-arc Basin. *Earth Planet. Sci. Lett.* 369–370:13–23
- Porcelli D, Wasserburg G. 1995. Mass transfer of helium, neon, argon, and xenon through a steady-state upper mantle. *Geochim. Cosmochim. Acta* 59:4921–37
- Porcelli D, Wollun D, Cassen P. 2001. Deep Earth rare gases: initial inventories, capture from the solar nebula, and losses during Moon formation. *Earth Planet. Sci. Lett.* 193:237–51

- Poreda RJ, Farley KA. 1992. Rare gases in Samoan xenoliths. *Earth Planet. Sci. Lett.* 113:129–44
- Pujol M, Marty B, Burgess R. 2011. Chondritic-like xenon trapped in Archean rocks: a possible signature of the ancient atmosphere. *Earth Planet. Sci. Lett.* 308:298–30
- Raquin A, Moreira M. 2009. Atmospheric  $^{38}\text{Ar}/^{36}\text{Ar}$  in the mantle: implications for the nature of the terrestrial parent bodies. *Earth Planet. Sci. Lett.* 287:551–58
- Raquin A, Moreira M, Guillon F. 2008. He, Ne and Ar systematics in single vesicles: mantle isotopic ratios and origin of the air component in basaltic glasses. *Earth Planet. Sci. Lett.* 274:142–50
- Rubie DC, Jacobson SA, Morbidelli A, O'Brien DP, Young ED, et al. 2015. Accretion and differentiation of the terrestrial planets with implications for the compositions of early-formed Solar System bodies and accretion of water. *Icarus* 248:89–108
- Sarda P, Moreira M, Staudacher T. 2000. Rare gas systematics on the southernmost Mid-Atlantic Ridge: constraints on the lower mantle and the Dupal source. *J. Geophys. Res.* 105(B3):5973–96
- Sarda P, Staudacher T, Allègre CJ. 1988. Neon isotopes in submarine basalts. *Earth Planet. Sci. Lett.* 91:73–88
- Schlichting HE, Mukhopadhyay S. 2018. Atmospheric impact losses. *Space Sci. Rev.* 214:34
- Schlichting HE, Sari R, Yalinewich A. 2015. Atmospheric mass loss during planet formation: the importance of planetesimals impacts. *Icarus* 247:81–94
- Schonbachler M, Carlson RW, Horan MF, Mock TD, Hauri EH. 2010. Heterogeneous accretion and the moderately volatile element budget of Earth. *Science* 328:884–87
- Sharp ZD. 2017. Nebular ingassing as a source of volatiles to the terrestrial planets. *Chem. Geol.* 448:137–50
- Sharp ZD, Draper DS. 2013. The chlorine abundance of Earth: implications for a habitable planet. *Earth Planet. Sci. Lett.* 369–370:71–77
- Shcheka SS, Keppler H. 2012. The origin of the terrestrial noble-gas signature. *Nature* 490:531–34
- Solomatov V. 2000. Fluid dynamics of magma oceans. In *Origin of the Earth and Moon*, ed. R Canup, K Righter, pp. 323–38. Tucson, AZ: Univ. Arizona Press
- Šrámek O, Stevens L, McDonough WF, Mukhopadhyay S, Peterson RJ. 2017. Subterranean production of neutrons,  $^{39}\text{Ar}$  and  $^{21}\text{Ne}$ : rates and uncertainties. *Geochim. Cosmochim. Acta* 196:370–87
- Staudacher T, Allègre CJ. 1982. Terrestrial xenology. *Earth Planet. Sci. Lett.* 60:389–406
- Staudacher T, Allègre CJ. 1988. Recycling of oceanic crust and sediments: the noble gas subduction barrier. *Earth Planet. Sci. Lett.* 89:173–83
- Staudacher T, Sarda P, Allègre CJ. 1986. New noble-gas data on glass samples from Loihi seamount and Hualalai and on dunite samples from Loihi and Reunion Island. *Chem Geol.* 56:193–205
- Stuart FM, Lass-Evans S, Fitton JG, Ellam RM. 2003. High  $^3\text{He}/^4\text{He}$  ratios in picritic basalts from Baffin Island and the role of a mixed reservoir in mantle plumes. *Nature* 424:57–59
- Sumino H, Burgess R, Mizukami T, Wallis SR, Holland G, Ballentine CJ. 2010. Seawater-derived noble gases and halogens preserved in exhumed mantle wedge peridotite. *Earth Planet. Sci. Lett.* 294:163–72
- Tang H, Dauphas N. 2014. The  $^{60}\text{Fe}$ - $^{60}\text{Ni}$ -chronology of core formation in Mars. *Earth Planet. Sci. Lett.* 390:264–74
- Thomas CW, Liu Q, Agee CB, Asimow PD, Lange RA. 2012. Multi-technique equation of state for  $\text{Fe}_2\text{SiO}_4$  melt and the density of Fe-bearing silicate melts from 0 to 161 GPa. *J. Geophys. Res.* 117(B10):B10206
- Tolstikhin IN, Hofmann AW. 2005. Early crust on top of the Earth's core. *Phys. Earth Planet. Inter.* 148:109–30
- Tolstikhin IN, Kramers JD, Hofmann AW. 2006. A chemical Earth model with whole mantle convection: the importance of a core–mantle boundary layer ( $D''$ ) and its early formation. *Chem. Geol.* 226:79–99
- Tolstikhin IN, O'Nions RK. 1996. Some comments on isotopic structure of terrestrial xenon. *Chem. Geol.* 129:185–99
- Trieloff M, Kunz J. 2005. Isotope systematics of noble gases in the Earth's mantle: possible sources of primordial isotopes and implications for mantle structure. *Phys. Earth Planet. Inter.* 148:13–38
- Trieloff M, Kunz J, Allègre CJ. 2002. Noble gas systematics of the Réunion mantle plume source and the origin of primordial noble gases in Earth's mantle. *Earth Planet. Sci. Lett.* 200:297–313
- Trieloff M, Kunz J, Clague DA, Harrison D, Allègre CJ. 2000. The nature of pristine noble gases in mantle plumes. *Science* 288:1036–38
- Tucker JM, Mukhopadhyay S. 2014. Evidence for multiple magma ocean outgassing and atmospheric loss episodes from mantle noble gases. *Earth Planet. Sci. Lett.* 393:254–65

- Tucker JM, Mukhopadhyay S, Gonnermann HM. 2018. Reconstructing mantle carbon and noble gas contents from degassed mid-ocean ridge basalts. *Earth Planet. Sci. Lett.* 496:108–19
- Tucker JM, Mukhopadhyay S, Schilling JG. 2012. The heavy noble gas composition of the depleted MORB mantle (DMM) and its implications for the preservation of heterogeneities in the mantle. *Earth Planet. Sci. Lett.* 355:244–54
- van Keken PE, Ballentine CJ. 1998. Whole-mantle versus layered mantle convection and the role of a high-viscosity lower mantle in terrestrial volatile evolution. *Earth Planet. Sci. Lett.* 156:19–32
- van Keken PE, Ballentine CJ. 1999. Dynamical models of mantle volatile evolution and the role of phase transitions and temperature-dependent rheology. *J. Geophys. Res.* 104(B4):7137–51
- Walsh KJ, Morbidelli A, Raymond SN, O'Brien DP, Mandell AM. 2011. A low mass for Mars from Jupiter's early gas-driven migration. *Nature* 475:206–9
- Wieler R. 1994. "Q-gases" as "local" primordial noble gas component in primitive meteorites. In *Noble Gas Geochemistry and Cosmochemistry*, ed. J Matsuda, pp. 31–41. Tokyo: Terra Sci. Publ.
- Wyatt MC. 2008. Evolution of debris disks. *Annu. Rev. Astron. Astrophys.* 46:339–83
- Yin Q, Jacobsen SB, Yamashita K, Blichert-Toft J, Télouk P, Albarède F. 2001. A short timescale for terrestrial planet formation from Hf-W chronometry of meteorites. *Nature* 418:949–52
- Yokochi R, Marty B. 2004. A determination of the neon isotopic composition of the deep mantle. *Earth Planet. Sci. Lett.* 225:77–88

## Contents

Big Time <i>Paul F. Hoffman</i> .....	1
Unanticipated Uses of the Global Positioning System <i>Kristine M. Larson</i> .....	19
Dynamics in the Uppermost Lower Mantle: Insights into the Deep Mantle Water Cycle Based on the Numerical Modeling of Subducted Slabs and Global-Scale Mantle Dynamics <i>Takashi Nakagawa and Tomoeki Nakakuki</i> .....	41
Atmospheric Escape and the Evolution of Close-In Exoplanets <i>James E. Owen</i> .....	67
The Sedimentary Cycle on Early Mars <i>Scott M. McLennan, John P. Grotzinger, Joel A. Hurowitz, and Nicholas J. Tosca</i> .....	91
New Horizons Observations of the Atmosphere of Pluto <i>G. Randall Gladstone and Leslie A. Young</i> .....	119
The Compositional Diversity of Low-Mass Exoplanets <i>Daniel Jontof-Hutter</i> .....	141
Destruction of the North China Craton in the Mesozoic <i>Fu-Yuan Wu, Jin-Hui Yang, Yi-Gang Xu, Simon A. Wilde, and Richard J. Walker</i> .....	173
Seawater Chemistry Through Phanerozoic Time <i>Alexandra V. Turchyn and Donald J. DePaolo</i> .....	197
Global Patterns of Carbon Dioxide Variability from Satellite Observations <i>Xun Jiang and Yuk L. Yung</i> .....	225
Permeability of Clays and Shales <i>C.E. Neuzil</i> .....	247
Flood Basalts and Mass Extinctions <i>Matthew E. Clapham and Paul R. Renne</i> .....	275
Repeating Earthquakes <i>Naoki Uchida and Roland Bürgmann</i> .....	305

Soil Functions: Connecting Earth's Critical Zone <i>Steven A. Banwart, Nikolaos P. Nikolaidis, Yong-Guan Zhu, Caroline L. Peacock, and Donald L. Sparks</i> .....	333
Earthquake Early Warning: Advances, Scientific Challenges, and Societal Needs <i>Richard M. Allen and Diego Melgar</i> .....	361
Noble Gases: A Record of Earth's Evolution and Mantle Dynamics <i>Sujoy Mukhopadhyay and Rita Parai</i> .....	389
Supraglacial Streams and Rivers <i>Lincoln H Pitcher and Laurence C. Smith</i> .....	421
Isotopes in the Water Cycle: Regional- to Global-Scale Patterns and Applications <i>Gabriel J. Bowen, Zhongyin Cai, Richard P. Fiorella, and Annie L. Putman</i> .....	453
Marsh Processes and Their Response to Climate Change and Sea-Level Rise <i>Duncan M. FitzGerald and Zoe Hughes</i> .....	481
The Mesozoic Biogeographic History of Gondwanan Terrestrial Vertebrates: Insights from Madagascar's Fossil Record <i>David W. Krause, Joseph J.W. Sertich, Patrick M. O'Connor, Kristina Curry Rogers, and Raymond R. Rogers</i> .....	519
Droughts, Wildfires, and Forest Carbon Cycling: A Pantropical Synthesis <i>Paulo M. Brando, Lucas Paolucci, Caroline C. Ummenhofer, Elsa M. Ordway, Henrik Hartmann, Megan E. Cattau, Ludmila Rattis, Vincent Medjibe, Michael T. Coe, and Jennifer Balch</i> .....	555
Exoplanet Clouds <i>Christiane Helling</i> .....	583

## Errata

An online log of corrections to *Annual Review of Earth and Planetary Sciences* articles may be found at <http://www.annualreviews.org/errata/earth>